Predictive current control in electrical drives: an illustrated review with case examples using a five-phase induction motor drive with distributed windings

Mario Bermúdez[1], Cristina Martín[2], Ignacio González-Prieto[3], Mario J. Durán[3], Manuel R. Arahal[4], Federico Barrero[2,]*

[1] *Electrical Engineering Department, University of Huelva, Avenida de las Fuerzas Armadas s/n, 21007, Huelva, Spain*
[2] *Electronic Engineering Department, University of Sevilla, Camino de los Descubrimientos s/n, 41092, Sevilla, Spain*
[3] *Electrical Engineering Department, University of Málaga, C/ Doctor Ortiz Ramos s/n, 29071, Málaga, Spain*
[4] *Systems Engineering and Automation Department, University of Sevilla, Camino de los Descubrimientos s/n, 41092, Sevilla, Spain*
[*] fbarrero@us.es

Abstract: The industrial application of electric machines in variable-speed drives has grown in the last decades thanks to the development of microprocessors and power converters. Although three-phase machines constitute the most common case, the interest of the research community has been recently focused on machines with more than three phases, known as multiphase machines. The principal reason lies in the exploitation of their advantages like reliability, better current distribution among phases or lower current harmonic production in the power converter than conventional three-phase ones, to name a few. Nevertheless, multiphase drives applications require the development of complex controllers to regulate the torque (or speed) and flux of the machine. In this regard, predictive current controllers have recently appeared as a viable alternative due to an easy formulation and a high flexibility to incorporate different control objectives. It is found however that these controllers face some peculiarities and limitations in their use that require attention. This work attempts to tackle the predictive current control technique as a viable alternative for the regulation of multiphase drives, paying special attention to the development of the control technique and the discussion of the benefits and limitations. Case examples with experimental results in a symmetrical five-phase induction machine with distributed windings in motoring mode of operation are used to this end.

1. Introduction

It is expected that 80% of all the produced energy will be used by electric drives by 2030. Electric vehicles play a major role in this context, as they will account for almost 50% of the automotive market by that year [1]. Furthermore, electric drives are the basis of locomotive traction, electric ship propulsion, more-electric aircraft for various auxiliary functions (e.g., fuel pumps, starter/generator solutions, etc.), and renewable energy production. While conventional three-phase drives represent the principal choice for industrial applications, multiphase ones have recently awoken the interest of practitioners and researchers in the field.

Any energy conversion system formed by a multiphase electric machine supplied from a multi-channel converter is termed multiphase drive. The first application of such a system was done in the late 60s in a five-phase drive [2], showing some of the advantages of multiphase systems over conventional three-phase ones. The main interest of this proposal was to highlight that the higher number of phases yields a torque ripple three-times lower with respect to the equivalent three-phase case. The better power distribution per phase helped in this way to mitigate one of the most reported problems in conventional drives by that time. However, it was not until the beginning of the 21st century that the interest of researchers in multiphase machines was renewed due to two main reasons. Firstly, the development of high-power high-frequency semiconductors using Pulse Wide Modulation (PWM) methods to control the ON/OFF states of these electronic devices. Secondly, the development of the microelectronic technology and the appearance of Digital Signal Processors (DSPs) and Field-Programmable Gate Arrays (FPGAs) with the ability to implement control algorithms in real time.

Notwithstanding the foregoing, the crucial reasons for the renewed interest in multiphase drives can also be found in their intrinsic advantages together with the discovery of innovative and exclusive modes of operation. These benefits are based on the extra degrees of freedom provided by the higher number of phases, and are mainly the following:

- The fault-tolerant capability against a fault situation in the machine and/or the power converter, firstly presented in [3]. An *n*-phase machine can operate after one or several fault occurrences without any external equipment, as long as the number of healthy phases remains greater than or equal to three (assuming a single isolated neutral connection). Consequently, the system reliability is enhanced at the expense of a reduction in the post-fault electrical torque production.
- The capability to increase the power density in healthy operation by injecting specific current harmonics, firstly exposed in [4]. This is possible in certain multiphase machine configurations based on concentrated windings, where the lower current harmonic components can be used to increase the torque production.

These advances and advantages underlie the adoption of multiphase machines for variable-speed drives in specific industry applications [5,6]. Electric propulsion of ships, traction in electric vehicles (hybrid/electric vehicles and locomotives), wind energy generation and low-power electric systems for more-electric aircraft are fields where the investigation in the last 20 years has been focused on [7,8]. The interest of multiphase machines in the cited applications, instead of their conventional three-phase counterparts, arises from the high torque/current and/or fault-tolerant requirements. Benchmark solutions adopted by important companies are the ultrahigh-speed elevator of Hyundai based on a 1.1 MW nine-phase electric drive [9] (see Fig. 1), the 5 MW twelve-phase electric drives in the wind turbines of Gamesa for onshore and offshore plants, and the 20 MW fifteen-phase electric drive for ship propulsion introduced by the GE Power Conversion company in the Royal Navy [10].

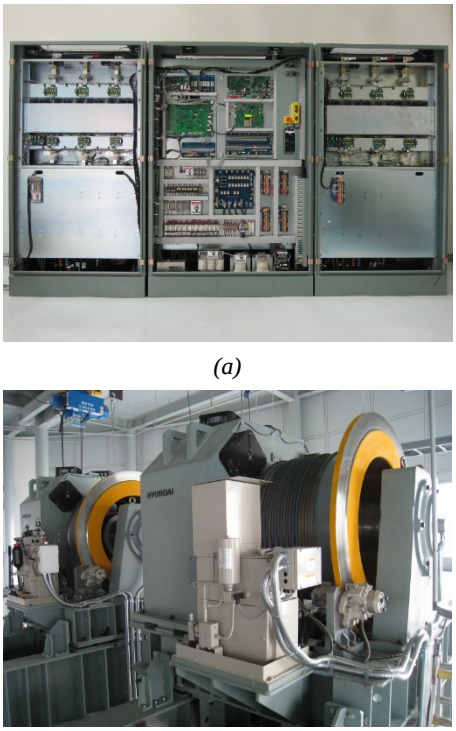

(a)

(b)

Fig. 1. *Example of an industrial multiphase drive: the ultrahigh-speed elevator developed by Hyundai, based on (a) multiple three-phase back-to-back converters and (b) a nine-phase permanent magnet synchronous machine with three isolated neutral points*

In order to create a body of knowledge, recent research works review the advances in the field of multiphase drives including their industrial applications, machine design and modeling, types of converters, modulation techniques, control strategies and innovative uses of the additional degrees of freedom (i.e., multimotor drives, battery chargers, post-fault control or dynamic breaking) [10,11-13]. In general terms, they show that: *i*) symmetrical five-phase and asymmetrical six-phase machines with isolated neutrals are the most popular multiphase machine types in the research community, and *ii*) an evolution in the control techniques has been necessary in order to optimally exploit their inherent advantages. In this regard, asymmetrical six-phase machines with isolated neutrals can be considered as two conventional three-phase machines coupled in a common case, while the five-phase drive can be considered the ideal case example to illustrate any study in the multiphase drive field. Previous state-of-the-art analyses on multiphase drives set the advances in the area in the last decades. However, they are mainly aimed at researchers and lack important information for practitioners and researchers starting in the field.

Field Oriented and Direct Torque Controllers (FOC and DTC, respectively) have been usually considered as standard regulation strategies in conventional three-phase drives. However, Model Predictive Controllers (MPC) have recently appeared as a promising alternative. The simplicity and intuitive formulation of the control problem using predictive controllers applied to electric drives has boosted the interest of the research community [10,11-13]. This is particularly true in the multiphase drives field, where predictive controllers offer the possibility to perform multi-objective and multi-variable control, including non-linearities or constraints into the control process by just defining a proper cost function. Nevertheless, MPC faces some limitations that still require attention, being the most prominent one a high computational cost, which increases with the number of phases.

This manuscript presents an up-to-date review of the most recent research in relation to the use of predictive current controllers for multiphase machines. The work goes beyond previous published papers, not only including the most recent applications of this technique found in literature, but also identifying some future research trends in the area. Furthermore, a detailed illustration using a particular five-phase induction motor drive as case example constitutes the basis of the review, with the aim of providing, all in all, a framework of analysis and guidelines for researchers and practitioners. After this introductory section, the paper is organized as follows. First, the five-phase induction motor drive system, which will be used as a case example along the work, is analyzed and modeled. Next, the control techniques recently used in multiphase drives are reviewed, focusing on the Predictive Current Control approach but in the context of control techniques that have been extended to multiphase drives in recent times. The key design and implementation features in predictive controllers, as well as the future prospect in the field are shown in Sections 4 and 5, respectively, and the conclusions are finally drawn in the last section of the manuscript.

2. Multiphase drives: the case of five-phase IM drives with distributed windings

A common feature in most control techniques applied to multiphase drives, particularly MPC methods, is the necessity of a precise and complete knowledge of the system dynamics through a mathematical model. To obtain that model, different construction aspects of the multiphase machine and the power converter must be taken into account, beginning with the type of machine and converter.

Depending on the rotor construction, multiphase machines can be divided into two main types, multiphase induction machines (IM) and multiphase synchronous machines, usually of the permanent magnet type (PMSM). Although both types present similar modeling approaches, IMs benefit from a simple and rugged construction with cheaper materials, low maintenance requirements, and well-proven technology, making them a usual election in industrial applications. Concerning the winding arrangement, the division is done between symmetrical or asymmetrical multiphase machines. First ones are constituted by consecutive phase windings equally displaced $2\pi/n$ (being n the number of phases), whereas the second ones are typically formed by independent sets of windings displaced π/n. Another classification considers the number of phases, distinguishing between machines with an odd or an even number of phases, and machines with multiple sets of three-phase windings. Notice that the higher the number of phases, the more complex the model. Finally, multiphase machines can be constructed with either concentrated or distributed windings. The most relevant interest in the concentrated-windings type is the existence of higher-order spatial harmonics in the magneto-motive force (MMF) that contribute to the electrical torque enhancement. Conversely, these harmonics can be neglected in distributed-windings machines (with an appropriate stator winding design), resulting in near sinusoidal MMF.

Regarding the power converter topology, the most widespread option is the back-to-back configuration, usually formed by a grid-connected three-phase rectifier electrically coupled to an *n*-phase inverter through a DC-link. This configuration permits the independent regulation of the inverter stage since it is decoupled from the distribution grid. Furthermore, it presents the capacity to generate an output with a wide range of frequencies and a small content of low-order harmonics by means of a suitable control algorithm (principally PWM-based techniques). The most used inverter type is the IGBT-based two-level voltage source inverter (VSI) that single-sided supplies the electric machine. However, depending on the application requirements, other types and converter topologies (multilevel VSI, matrix VSI or even current source inverters) can be found in the literature [14-16].

The model of the multiphase drive used as case example, composed by a five-phase two-level VSI that supplies a symmetrical five-phase IM with distributed windings, is introduced here. First, the physical model of the induction machine is presented, covering the one based on phase variables (or original model), and the

additional transformations conventionally applied to reduce the complexity of the mathematical equations. These are the decoupled (Clarke) transformation and the rotational (Park) transformation. Finally, the model of the power converter is also presented.

2.1. Five-phase IM machine with distributed windings

Any multiphase machine can be described as a set of differential equations in phase variables (currents, voltages and fluxes) using the general theory of electric machines [17]. However, the generalization from Fortescue and Clarke [18,19] laid the foundations for different mathematical transformations. Their main objective is the replacement of the original phase-variable model by equivalent equations using a reduced set of new (fictitious) variables, thus permitting the simplification of the machine model. These transformations are collected in what is usually named Vector Space Decomposition (VSD) approach [20,21], where matrix representation is conventionally adopted. This approach is slightly different depending on the winding arrangement of the machine (symmetrical or asymmetrical, and distributed or concentrated) and on the number of phases (multiple of three or not). Therefore, multiple works have been developed in the field of multiphase machines modeling, considering different topologies of both induction and synchronous machines [4,11,22-24].

The focus here is the symmetrical five-phase induction machine with distributed windings that are electrically displaced by $\vartheta = 2\pi/5$. Since the rotor is squirrel-cage type, it can be treated as five windings equally displaced $\vartheta = 2\pi/5$ around the rotor circumference. A schematic representation of the machine is presented in Fig. 2, where s_a to s_e and r_a to r_e denote each phase of the stator and rotor windings, respectively. These windings are star-connected with an isolated neutral point. Additional simplifying assumptions are considered in the modeling:

- All phase windings in the stator/rotor are considered identical.
- The distribution of the MMF and, consequently, the flux around the air-gap can be regarded as sinusoidal, assuming symmetrical distributed windings. This means that all spatial harmonics can be neglected, except for the fundamental one.
- The magnetization characteristic of the ferromagnetic material is assumed to be linear. Therefore, the effects of magnetic field saturation are negligible and mutual inductances are constant.
- The air-gap is regarded as uniform by neglecting the impact of slotting.
- Stator and rotor resistances and leakage inductances are considered constant. Variations due to temperature and/or skin effect are neglected.
- Losses in the ferromagnetic material due to hysteresis and eddy currents are not considered.

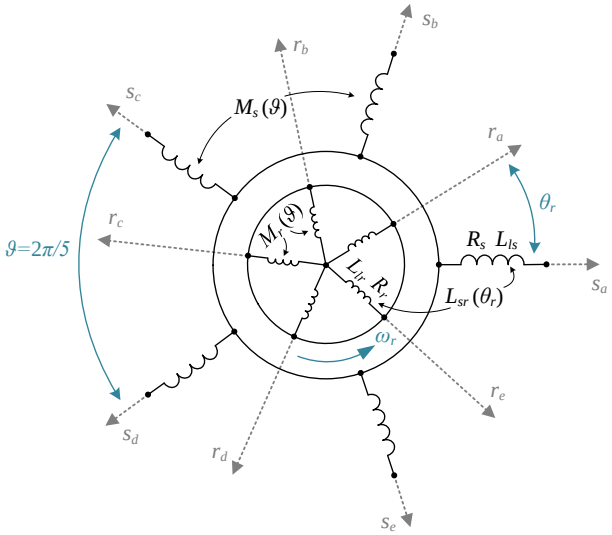

Fig. 2. *Scheme of the symmetrical and distributed-windings five-phase IM*

Taking into account the previous hypotheses and considering that the positive direction for the currents is from the supply source to the machine phases (motoring convention), the stator and rotor voltage equilibrium equations that describe each phase of the machine can be expressed in the following matrix form:

$$\boldsymbol{v_s} = R_s \boldsymbol{i_s} + \frac{d\boldsymbol{\lambda_s}}{dt}$$

$$\boldsymbol{v_r} = R_r \boldsymbol{i_r} + \frac{d\boldsymbol{\lambda_r}}{dt} \tag{1}$$

where R_s and R_r are the stator and rotor resistances. Stator and rotor currents ($\boldsymbol{i}$), voltages ($\boldsymbol{v}$) and fluxes ($\boldsymbol{\lambda}$) are defined as

$$\boldsymbol{v_s} = [v_{sa}\ v_{sb}\ v_{sc}\ v_{sd}\ v_{se}]^T$$

$$\boldsymbol{i_s} = [i_{sa}\ i_{sb}\ i_{sc}\ i_{sd}\ i_{se}]^T$$

$$\boldsymbol{\lambda_s} = [\lambda_{sa}\ \lambda_{sb}\ \lambda_{sc}\ \lambda_{sd}\ \lambda_{se}]^T$$

$$\boldsymbol{v_r} = [v_{ra}\ v_{rb}\ v_{rc}\ v_{rd}\ v_{re}]^T$$

$$\boldsymbol{i_r} = [i_{ra}\ i_{rb}\ i_{rc}\ i_{rd}\ i_{re}]^T$$

$$\boldsymbol{\lambda_r} = [\lambda_{ra}\ \lambda_{rb}\ \lambda_{rc}\ \lambda_{rd}\ \lambda_{re}]^T. \tag{2}$$

Since the studied induction machine has a squirrel-cage topology, rotor voltages are equal to zero. Additionally, it is important to remark that rotor variables and parameters in (1) and (2) are referred to the stator, this being a common procedure in three-phase machine modeling. Previous equations are completed with the definition of the stator and rotor fluxes in terms of stator and rotor currents (3), which represent the coupling between the stator and rotor.

$$\boldsymbol{\lambda_s} = \boldsymbol{L_s i_s} + \boldsymbol{L_{sr}}(\theta_r)\boldsymbol{i_r}$$

$$\boldsymbol{\lambda_r} = \boldsymbol{L_r i_r} + \boldsymbol{L_{rs}}(\theta_r)\boldsymbol{i_s}. \tag{3}$$

Under the above considerations, stator and rotor inductance matrices, $\boldsymbol{L_s}$ and $\boldsymbol{L_r}$, have constant coefficients that only depend on the stator and rotor leakage inductances L_{ls} and L_{lr}, the mutual inductance M, and the winding electrical displacement ϑ as follows:

$$\boldsymbol{L_s} = L_{ls}\boldsymbol{I_5} + \boldsymbol{M_s}(\vartheta)$$

$$\boldsymbol{L_r} = L_{lr}\boldsymbol{I_5} + \boldsymbol{M_r}(\vartheta)$$

$$\boldsymbol{M_s}(\vartheta) = \boldsymbol{M_r}(\vartheta) = M\begin{bmatrix} 1 & \cos(\vartheta) & \cos(2\vartheta) & \cos(3\vartheta) & \cos(4\vartheta) \\ \cos(4\vartheta) & 1 & \cos(\vartheta) & \cos(2\vartheta) & \cos(3\vartheta) \\ \cos(3\vartheta) & \cos(4\vartheta) & 1 & \cos(\vartheta) & \cos(2\vartheta) \\ \cos(2\vartheta) & \cos(3\vartheta) & \cos(4\vartheta) & 1 & \cos(\vartheta) \\ \cos(\vartheta) & \cos(2\vartheta) & \cos(3\vartheta) & \cos(4\vartheta) & 1 \end{bmatrix}. \tag{4}$$

On the other hand, mutual stator-to-rotor and rotor-to-stator inductance matrices in (3), which verify that $\boldsymbol{L_{sr}}(\theta_r) = \boldsymbol{L_{rs}}(\theta_r)^T$, are not constant but dependent on the instantaneous value of the rotor position with respect to the stator, θ_r, through

$$\boldsymbol{L_{sr}}(\theta_r) = M\begin{bmatrix} \cos(\Delta_0) & \cos(\Delta_1) & \cos(\Delta_2) & \cos(\Delta_3) & \cos(\Delta_4) \\ \cos(\Delta_4) & \cos(\Delta_0) & \cos(\Delta_1) & \cos(\Delta_2) & \cos(\Delta_3) \\ \cos(\Delta_3) & \cos(\Delta_4) & \cos(\Delta_0) & \cos(\Delta_1) & \cos(\Delta_2) \\ \cos(\Delta_2) & \cos(\Delta_3) & \cos(\Delta_4) & \cos(\Delta_0) & \cos(\Delta_1) \\ \cos(\Delta_1) & \cos(\Delta_2) & \cos(\Delta_3) & \cos(\Delta_4) & \cos(\Delta_0) \end{bmatrix} \tag{5}$$

where $\Delta_k = \theta_r + k\vartheta$, with k = 1,2,...,5; and the rotor angle is obtained through the electrical rotor speed

$$\theta_r = \int_0^t \omega_r dt. \tag{6}$$

Equations (1)-(6) describe the electrical part of the five-phase IM that is complemented with the mechanical equation

$$J_m \frac{d\omega_m}{dt} + B_m \omega_m = T_e - T_L \tag{7}$$

being ω_m the mechanical speed of the rotor shaft ($\omega_r = P\omega_m$, with P the number of pole pairs), T_L the load torque applied to the machine, T_e the electromagnetic torque, J_m the inertia of the rotating masses, and B_m the friction coefficient. The electromagnetic torque is responsible for the electromechanical energy conversion, linking the electrical and mechanical subsystems. This torque is obtained with the following equation:

$$T_e = \frac{P}{2}\begin{bmatrix}\boldsymbol{i_s}\\ \boldsymbol{i_r}\end{bmatrix}^T \frac{d}{d\theta_r}\begin{bmatrix}\boldsymbol{L_s} & \boldsymbol{L_{sr}}(\theta_r)\\ \boldsymbol{L_{rs}}(\theta_r) & \boldsymbol{L_r}\end{bmatrix}\begin{bmatrix}\boldsymbol{i_s}\\ \boldsymbol{i_r}\end{bmatrix}. \tag{8}$$

Taking into account that stator and rotor inductance matrices do not depend on the rotor position, the previous equation can be reduced to the one in (9), where it can be observed that the electromagnetic torque is entirely created from the interaction between the stator and rotor.

$$T_e = \frac{P}{2}\boldsymbol{i_s}^T \frac{d\boldsymbol{L_{sr}}(\theta_r)}{d\theta_r}\boldsymbol{i_r}. \tag{9}$$

To summarize, the five-phase IM can be represented in the phase-variable domain through $2n + 1 = 11$ first-order differential equations, after the substitution of the flux expressions (3) into the voltage equilibrium equations (1), and the electromagnetic torque value (9) into the mechanical equation (7); plus 1 integral equation (6). Due to the time-dependence through the rotor position angle, these equations constitute a non-linear time-variant system.

Even if the resolution of the phase-variable equations is possible with advanced computational devices, important simplifications can be done through the VSD approach. Thus, it is possible to represent the five-phase IM model in a stationary reference frame formed by a new set of five fictitious variables using the Clarke transformation. They are grouped into two two-dimensional orthogonal planes, named *α-β* and *x-y*, whose components are also orthogonal between them; plus an additional axis that contains the homopolar component, named *z*. The main characteristic of this new reference frame is that the different planes are completely decoupled due to the orthogonality, resulting in a simpler model that is more suitable for control purposes. In addition, the transformation of the phase variables into the new stationary reference frame provides better insight into the physical phenomena involved in the energy conversion process: the *α-β* plane becomes responsible for the torque production, while the *x-y* plane and the *z*-axis are only related to harmonic components and stator losses in the machine.

Then, the relationship between the original phase variables and the new fictitious ones is obtained by applying the decoupled (Clarke) transformation matrix $\boldsymbol{T_c}$, defined in (11), to the stator and the rotor variables in the following way:

$$\begin{aligned}
\begin{bmatrix}v_{s\alpha}\ v_{s\beta}\ v_{sx}\ v_{sy}\ v_{sz}\end{bmatrix}^T &= \boldsymbol{T_c}\boldsymbol{v_s}\\
\begin{bmatrix}i_{s\alpha}\ i_{s\beta}\ i_{sx}\ i_{sy}\ i_{sz}\end{bmatrix}^T &= \boldsymbol{T_c}\boldsymbol{i_s}\\
\begin{bmatrix}\lambda_{s\alpha}\ \lambda_{s\beta}\ \lambda_{sx}\ \lambda_{sy}\ \lambda_{sz}\end{bmatrix}^T &= \boldsymbol{T_c}\boldsymbol{\lambda_s}\\
\begin{bmatrix}v_{r\alpha}\ v_{r\beta}\ v_{rx}\ v_{ry}\ v_{rz}\end{bmatrix}^T &= \boldsymbol{T_c}\boldsymbol{v_r}\\
\begin{bmatrix}i_{r\alpha}\ i_{r\beta}\ i_{rx}\ i_{ry}\ i_{rz}\end{bmatrix}^T &= \boldsymbol{T_c}\boldsymbol{i_r}\\
\begin{bmatrix}\lambda_{r\alpha}\ \lambda_{r\beta}\ \lambda_{rx}\ \lambda_{ry}\ \lambda_{rz}\end{bmatrix}^T &= \boldsymbol{T_c}\boldsymbol{\lambda_r}.
\end{aligned} \tag{10}$$

$$\boldsymbol{T_c} = \frac{2}{5}\begin{bmatrix}1 & \cos(\vartheta) & \cos(2\vartheta) & \cos(3\vartheta) & \cos(4\vartheta)\\ 0 & \sin(\vartheta) & \sin(2\vartheta) & \sin(3\vartheta) & \sin(4\vartheta)\\ 1 & \cos(2\vartheta) & \cos(4\vartheta) & \cos(6\vartheta) & \cos(8\vartheta)\\ 0 & \sin(2\vartheta) & \sin(4\vartheta) & \sin(6\vartheta) & \sin(8\vartheta)\\ 1/2 & 1/2 & 1/2 & 1/2 & 1/2\end{bmatrix}. \tag{11}$$

The coefficient $2/5$ in front of the transformation matrix is associated with the power of the machine after the transformation. The selected value keeps the original values of the electrical variables invariant after the transformation, but not the total power before and after the transformation, thus being commonly known as power-variant (or amplitude-invariant) transformation. However, it is also a common practice to use the coefficient $\sqrt{2/5}$ instead, which keeps the total power of the machine before and after the transformation invariant (power-invariant transformation [5]).

Substituting (3) into (1) and applying the decoupled transformation, the resultant stator and rotor equilibrium equations can be written as shown in (12) and (13) after some mathematical operations, where $L_m = (5/2)M$ is the equivalent mutual inductance, and the stator and rotor inductances in the new reference frame are defined as $L_s = L_{ls} + L_m$ and $L_r = L_{lr} + L_m$, respectively. The parameters that appear in these equations are, in essence, those of the well-known IM equivalent circuit in steady state. Consequently, they can be obtained from standard no-load and locked rotor tests [25,26].

$$\begin{aligned}
v_{s\alpha} &= R_s i_{s\alpha} + L_s \frac{di_{s\alpha}}{dt} + L_m \frac{d}{dt}\left(i'_{r\alpha}\cos\theta_r - i'_{r\beta}\sin\theta_r\right)\\
v_{s\beta} &= R_s i_{s\beta} + L_s \frac{di_{s\beta}}{dt} + L_m \frac{d}{dt}\left(i'_{r\alpha}\sin\theta_r + i'_{r\beta}\cos\theta_r\right)\\
v_{sx} &= R_s i_{sx} + L_{ls}\frac{di_{sx}}{dt}\\
v_{sy} &= R_s i_{sy} + L_{ls}\frac{di_{sy}}{dt}\\
v_{sz} &= R_s i_{sz} + L_{ls}\frac{di_{sz}}{dt}.
\end{aligned} \tag{12}$$

$$\begin{aligned}
v'_{r\alpha} = 0 &= R_r i'_{r\alpha} + L_r \frac{di'_{r\alpha}}{dt} + L_m \frac{d}{dt}\left(i_{s\alpha}\cos\theta_r - i_{s\beta}\sin\theta_r\right)\\
v'_{r\beta} = 0 &= R_r i'_{r\beta} + L_r \frac{di'_{r\beta}}{dt}\\
&\quad + L_m \frac{d}{dt}\left(-i_{s\alpha}\sin\theta_r + i_{s\beta}\cos\theta_r\right)\\
v_{rx} = 0 &= R_r i_{rx} + L_{lr}\frac{di_{rx}}{dt}\\
v_{ry} = 0 &= R_r i_{ry} + L_{lr}\frac{di_{ry}}{dt}\\
v_{rz} = 0 &= R_r i_{rz} + L_{lr}\frac{di_{rz}}{dt}.
\end{aligned} \tag{13}$$

Again, rotor voltages are considered zero since the rotor is squirrel-cage type. It can be seen that stator variables are referred to the stationary reference frame *α-β*, whereas rotor ones are referred to a different reference frame *α'-β'* that rotates at the rotor speed ω_r (see Fig. 3). This issue has been represented by the apostrophe in the rotor variables (v'_r and i'_r) only in the *α-β* equations because it is exclusively in this plane where the stator and rotor coupling takes place. As a consequence, the dependence on the rotor angle in some inductance terms still remains. In order to eliminate this dependence, it is necessary to apply an additional change of variables, which is

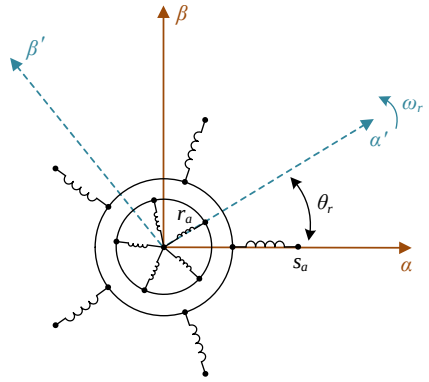

Fig. 3. *Reference frames of stator (α-β) and rotor (α'-β') variables*

equivalent to a rotational transformation of the rotor *α'-β'* variables into the stationary *α-β* plane. This is done using the following rotational matrix [5,6]:

$$\boldsymbol{T_r}(\theta_r) = \begin{bmatrix} \cos\theta_r & -\sin\theta_r \\ \sin\theta_r & \cos\theta_r \end{bmatrix}. \tag{14}$$

After the application of the rotational transformation to equations (12) and (13), the final electrical model of the machine in the stationary reference frame can be cast in the form [5,6]

$$v_{s\alpha} = R_s i_{s\alpha} + L_s \frac{di_{s\alpha}}{dt} + L_m \frac{di_{r\alpha}}{dt} = R_s i_{s\alpha} + \frac{d\lambda_{s\alpha}}{dt}$$

$$v_{s\beta} = R_s i_{s\beta} + L_s \frac{di_{s\beta}}{dt} + L_m \frac{di_{r\beta}}{dt} = R_s i_{s\beta} + \frac{d\lambda_{s\beta}}{dt}$$

$$v_{sx} = R_s i_{sx} + L_{ls} \frac{di_{sx}}{dt} = R_s i_{sx} + \frac{d\lambda_{sx}}{dt}$$

$$v_{sy} = R_s i_{sy} + L_{ls} \frac{di_{sy}}{dt} = R_s i_{sy} + \frac{d\lambda_{sy}}{dt}$$

$$v_{sz} = R_s i_{sz} + L_{ls} \frac{di_{sz}}{dt} = R_s i_{sz} + \frac{d\lambda_{sz}}{dt} \tag{15}$$

$$\begin{aligned} v_{r\alpha} = 0 &= R_r i_{r\alpha} + L_r \frac{di_{r\alpha}}{dt} + L_m \frac{di_{s\alpha}}{dt} + \omega_r \left(L_r i_{r\beta} + L_m i_{s\beta}\right) \\ &= R_r i_{r\alpha} + \frac{d\lambda_{r\alpha}}{dt} + \omega_r \lambda_{r\beta} \end{aligned}$$

$$\begin{aligned} v_{r\beta} = 0 &= R_r i_{r\beta} + L_r \frac{di_{r\beta}}{dt} + L_m \frac{di_{s\beta}}{dt} - \omega_r (L_r i_{r\alpha} + L_m i_{s\alpha}) \\ &= R_r i_{r\beta} + \frac{d\lambda_{r\beta}}{dt} - \omega_r \lambda_{r\alpha} \end{aligned}$$

$$v_{rx} = 0 = R_r i_{rx} + L_{lr} \frac{di_{rx}}{dt} = R_r i_{rx} + \frac{d\lambda_{rx}}{dt}$$

$$v_{ry} = 0 = R_r i_{ry} + L_{lr} \frac{di_{ry}}{dt} = R_r i_{ry} + \frac{d\lambda_{ry}}{dt}$$

$$v_{rz} = 0 = R_r i_{rz} + L_{lr} \frac{di_{rz}}{dt} = R_r i_{rz} + \frac{d\lambda_{rz}}{dt}. \tag{16}$$

Notice that new expressions for the rotor and stator fluxes have been deduced:

$$\lambda_{s\alpha} = L_s i_{s\alpha} + L_m i_{r\alpha} \qquad \lambda_{r\alpha} = L_r i_{r\alpha} + L_m i_{s\alpha}$$

$$\lambda_{s\beta} = L_s i_{s\beta} + L_m i_{r\beta} \qquad \lambda_{r\beta} = L_r i_{r\beta} + L_m i_{s\beta}$$

$$\lambda_{sx} = L_{ls} i_{sx} \qquad \lambda_{rx} = L_{lr} i_{rx}$$

$$\lambda_{sy} = L_{ls} i_{sy} \qquad \lambda_{ry} = L_{lr} i_{ry}$$

$$\lambda_{sz} = L_{ls} i_{sz} \qquad \lambda_{rz} = L_{lr} i_{rz}. \tag{17}$$

The electromagnetic torque (9) can be expressed in the new stationary reference frame applying (11) and (14), and performing some calculations, giving rise to the following expression [5,6]:

$$T_e = P \frac{5}{2} L_m (i_{r\alpha} i_{s\beta} - i_{r\beta} i_{s\alpha}). \tag{18}$$

It must be noted that the factor $5/2$ in this expression will not appear in the case of applying a power-invariant transformation. As expected, only variables in the *α-β* plane are involved in the electromechanical energy conversion process (remember that a distributed-winding machine is considered) or, in other words, in the fundamental torque and flux production.

Some additional analyses must be done regarding the electrical model in (15) and (16). Since the coupling between the rotor and stator windings exclusively takes place in the *α-β* plane, from the rotor voltage equations it can de deduced that *x-y* and *z* rotor voltages can be discarded. Furthermore, the star connection of the stator windings with isolated neutral points avoids the flow of the homopolar current, so there is no need to take into account the *z* component equation. After all these simplifications, the final machine model in the stationary reference frame can be totally described by 6 differential equations plus the mechanical equation with the new torque expression, which implies a significant reduction of the model complexity in comparison with the original phase-variable model. However, the non-linear and time-variant properties of the differential equations remain.

Note that the described transformation permits a detailed analysis of the voltage and current harmonic components, since some of them are mapped into certain planes. Therefore, in normal condition the fundamental frequency and harmonic components of order $10k \pm 1$, with $k = 1,2,3,\ldots,\infty$, map into the *α-β* plane contributing to the electromechanical energy conversion. Conversely, harmonics of order $10k \pm 3$ map into the *x-y* plane, only contributing to the losses in the machine. Finally, the DC component plus harmonics of order $5k$ map into the homopolar axis, which cannot flow in the case study.

Since *α-β* components are responsible for the torque/flux generation, they constitute the priority in the control process. However, these components present an oscillating nature, hence they are usually expressed in a rotating reference frame (termed *d-q*) to ease their regulation. Thus, after the rotational (Park) transformation, the *d-q* components of the electrical variables are constant in steady-state condition and variable during transients [27]. Regarding the *x-y* components, assuming an ideal symmetrical and balanced sinusoidal five-phase voltage supply, they are zero and consequently it is not necessary to rotate them. Nonetheless, they are also rotated in situations when the aforementioned assumption of ideal supply is no longer applicable (e.g., in fault conditions in the VSI legs [28]), leading to non-zero oscillating *x-y* currents.

In this transformation, the new *d-q* reference frame is considered to rotate at an arbitrary speed ω and its instantaneous position with respect to the stator *α-β* reference frame is defined by the electrical angle θ (see Fig. 4), being both quantities mutually related through

$$\theta = \int_0^t \omega \, dt. \tag{19}$$

Consequently, *α-β* stator variables can be referred to the new rotating reference frame with the following expressions and rotational matrix [5,6]:

$$\begin{bmatrix} v_{sd} & v_{sq} \end{bmatrix}^T = \boldsymbol{D_s}(\theta) \begin{bmatrix} v_{s\alpha} & v_{s\beta} \end{bmatrix}^T$$

$$\begin{bmatrix} i_{sd} & i_{sq} \end{bmatrix}^T = \boldsymbol{D_s}(\theta) \begin{bmatrix} i_{s\alpha} & i_{s\beta} \end{bmatrix}^T$$

$$\begin{bmatrix} \lambda_{sd} & \lambda_{sq} \end{bmatrix}^T = \boldsymbol{D_s}(\theta) \begin{bmatrix} \lambda_{s\alpha} & \lambda_{s\beta} \end{bmatrix}^T \tag{20}$$

$$\boldsymbol{D_s}(\theta) = \begin{bmatrix} cos\,\theta & sin\,\theta \\ -sin\,\theta & cos\,\theta \end{bmatrix}. \tag{21}$$

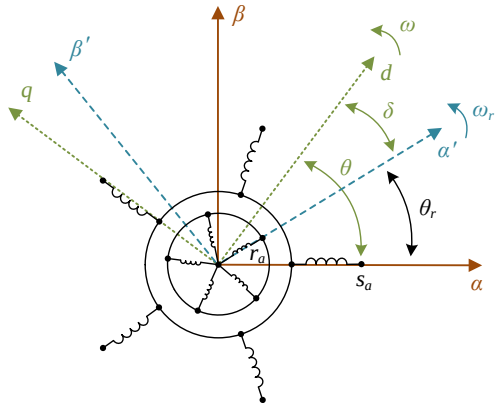

Fig. 4. *Rotating reference frame (d-q)*

In the case of rotor variables, expressed in the *α'-β'* plane after the Clarke transformation, a different rotational matrix must be defined in order to refer both stator and rotor variables to the same *d-q* reference frame, eliminating the relative motion between stator and rotor windings. Following the representation in Fig. 4, the instantaneous position of the rotor reference frame *α'-β'*, which rotates at the rotor speed ω_r, with respect to the *d-q* reference frame, is given by the electrical angle δ. This angle can be obtained through

$$\delta = \theta - \theta_r = \int_0^t (\omega - \omega_r)\, dt = \int_0^t \omega_{sl}\, dt \tag{22}$$

where ω_{sl} is the relative speed between the rotating and the rotor reference frames, called slip speed. Hence, the rotor variables in the new rotating reference frame are obtained using the following equations and rotational matrix:

$$\begin{bmatrix} v_{rd} & v_{rq} \end{bmatrix}^T = \boldsymbol{D_r}(\delta) \begin{bmatrix} v'_{r\alpha} & v'_{r\beta} \end{bmatrix}^T$$

$$\begin{bmatrix} i_{rd} & i_{rq} \end{bmatrix}^T = \boldsymbol{D_r}(\delta) \begin{bmatrix} i'_{r\alpha} & i'_{r\beta} \end{bmatrix}^T$$

$$\begin{bmatrix} \lambda_{rd} & \lambda_{rq} \end{bmatrix}^T = \boldsymbol{D_r}(\delta) \begin{bmatrix} \lambda'_{r\alpha} & \lambda'_{r\beta} \end{bmatrix}^T \tag{23}$$

$$\boldsymbol{D_r}(\theta) = \begin{bmatrix} cos\,\delta & sin\,\delta \\ -sin\,\delta & cos\,\delta \end{bmatrix}. \tag{24}$$

Applying the rotational matrices (21) and (24) to the stator and rotor voltage equilibrium equations (12) and (13), the complete machine model in the rotating reference frame can be expressed as

$$\begin{aligned} v_{sd} &= R_s i_{sd} + L_s \frac{di_{sd}}{dt} + L_m \frac{di_{rd}}{dt} - \omega\left(L_s i_{sq} + L_m i_{rq}\right) \\ &= R_s i_{sd} + \frac{d\lambda_{sd}}{dt} - \omega \lambda_{sq} \end{aligned}$$

$$\begin{aligned} v_{sq} &= R_s i_{sq} + L_s \frac{di_{sq}}{dt} + L_m \frac{di_{rq}}{dt} + \omega(L_s i_{sd} + L_m i_{rd}) \\ &= R_s i_{sq} + \frac{d\lambda_{sq}}{dt} + \omega \lambda_{sd} \end{aligned}$$

$$v_{sx} = R_s i_{sx} + L_{ls} \frac{di_{sx}}{dt} = R_s i_{sx} + \frac{d\lambda_{sx}}{dt}$$

$$v_{sy} = R_s i_{sy} + L_{ls} \frac{di_{sy}}{dt} = R_s i_{sy} + \frac{d\lambda_{sy}}{dt} \tag{25}$$

$$\begin{aligned} v_{rd} = 0 &= R_r i_{rd} + L_r \frac{di_{rd}}{dt} + L_m \frac{di_{sd}}{dt} - \omega_{sl}\left(L_r i_{rq} + L_m i_{sq}\right) \\ &= R_r i_{rd} + \frac{d\lambda_{rd}}{dt} - \omega_{sl} \lambda_{rq} \end{aligned}$$

$$\begin{aligned} v_{rq} = 0 &= R_r i_{rq} + L_r \frac{di_{rq}}{dt} + L_m \frac{di_{sq}}{dt} + \omega_{sl}(L_r i_{rd} + L_m i_{sd}) \\ &= R_r i_{rq} + \frac{d\lambda_{rq}}{dt} + \omega_{sl} \lambda_{rd} \end{aligned} \tag{26}$$

where the relationship between stator and rotor fluxes, and the stator and rotor currents in the rotating frame is the following:

$$\begin{aligned} \lambda_{sd} &= L_s i_{sd} + L_m i_{rd} & \lambda_{rd} &= L_r i_{rd} + L_m i_{sd} \\ \lambda_{sq} &= L_s i_{sq} + L_m i_{rq} & \lambda_{rq} &= L_r i_{rq} + L_m i_{sq} \\ \lambda_{sx} &= L_{ls} i_{sx} \\ \lambda_{sz} &= L_{ls} i_{sz}. \end{aligned} \tag{27}$$

Notice that equations in the *x-y* plane stay unaltered since the rotation is only performed in the *α-β* plane. For simplification purposes, the stator and rotor *z*-axis components and the rotor *x-y* components are omitted following the previous reasoning. Proceeding in an analogous way, a new expression of the electromagnetic torque can be derived [5,6]

$$T_e = P \frac{5}{2} L_m (i_{rd} i_{sq} - i_{rq} i_{sd}). \tag{28}$$

However, it is usual to find alternative expressions of this torque, such as the one shown in (29), where the correlation between stator and rotor fluxes and currents is implicitly considered. These alternative formulations are useful in some control strategies in order to reduce the number of calculations when the model is expressed in certain reference frames. Notice, again, that the $5/2$ coefficient would not appear if the power-invariant decoupling transformation is used instead of (11).

$$T_e = P \frac{5}{2} \left(\lambda_{sd} i_{sq} - \lambda_{sq} i_{sd}\right) = P \frac{5}{2} \frac{L_m}{L_r} (\lambda_{rd} i_{sq} - \lambda_{rq} i_{sd}). \tag{29}$$

As a final remark, the speed of the rotating reference frame (ω) can be arbitrarily selected in the IM. However, depending on the control strategy, some selections are more favorable than others to reduce the machine model complexity. This is the case of the Rotor Field Oriented Control (RFOC), where ω is selected in such a way that the *d*-axis is fixed to the rotor flux and, consequently, the projection of this flux in the *q*-axis becomes null [6,29]. Another considered option consists in the alignment of the reference frame to the stator flux, which is typically used in the DTC technique [30,31].

2.2. *The power converter model*

The simplest configuration corresponds to a two-level five-phase VSI, formed by two IGBTs per leg with their corresponding anti-parallel free-wheeling diodes, where the DC-link voltage (V_{dc}) is provided by an external low-impedance DC source. A schematic representation of this VSI is depicted in Fig. 5, where a balanced inductive load has been included to represent the machine stator windings when they are star-connected, being *N* the common neutral point. For this scheme, the state of each VSI leg can be defined as $S_j = \{0,1\}$, with $j = \{a,b,c,d,e\}$; being $S_j = 1$ when the upper IGBT is ON and the lower one is OFF, while the opposite occurs when $S_j = 0$. In this way, short circuits are avoided. In practice, a small dead-time should be introduced between the switching operation of the IGBTs aiming to avoid transient short circuits, but this is not reflected in the final VSI model for the sake of simplicity.

Under these considerations, the voltage v_j in the midpoint of the corresponding leg with respect to the negative bus of the DC-link can be defined in terms of the switching state of that leg using the following expression:

$$v_j = V_{dc} S_j. \tag{30}$$

This voltage is related to the stator phase voltage, v_{sj}, through the voltage between the common point of the star connection and the negative bus of the DC-link, v_N, in the following way:

$$v_j = v_{sj} + v_N. \tag{31}$$

Assuming a balanced load, the sum of the five stator phase voltages must be equal to zero. Thus, adding all stator phase voltages derived form (31) and combining the result with (30), the voltage v_N can be defined as

$$v_N = \frac{1}{5}\sum_{i=a}^{e} v_i = \frac{V_{dc}}{5}\sum_{i=a}^{e} S_i. \tag{32}$$

Introducing this value in (31), an expression for the stator phase voltages in terms of the switching states of the VSI legs can be derived

$$v_{sj} = v_j - v_N = V_{dc}S_j - \frac{V_{dc}}{5}\sum_{i=a}^{e} S_i = V_{dc}\left[S_j - \frac{1}{5}\sum_{i=a}^{e} S_i\right]. \tag{33}$$

Consequently, if the switching state of the VSI is defined as the vector $\boldsymbol{S} = [S_a\ S_b\ S_c\ S_d\ S_e]^T$, the above equation can be expressed in matrix form

$$\begin{bmatrix} v_{sa} \\ v_{sb} \\ v_{sc} \\ v_{sd} \\ v_{se} \end{bmatrix} = \frac{V_{dc}}{5}\begin{bmatrix} 4 & -1 & -1 & -1 & -1 \\ -1 & 4 & -1 & -1 & -1 \\ -1 & -1 & 4 & -1 & -1 \\ -1 & -1 & -1 & 4 & -1 \\ -1 & -1 & -1 & -1 & 4 \end{bmatrix}\begin{bmatrix} S_a \\ S_b \\ S_c \\ S_d \\ S_e \end{bmatrix}. \tag{34}$$

For the case of the five-phase configuration, there are $2^5 = 32$ possible switching states that lead to phase voltage values equal to 0, $\pm 1/5V_{dc}$, $\pm 2/5V_{dc}$, $\pm 3/5V_{dc}$ and $\pm 4/5V_{dc}$, according to (34). These states constitute different load conditions from the point of view of the VSI, characterized by the number of load windings connected to the positive and negative rails of the DC-link. The higher the number of phases of the VSI, the higher the number of voltage levels that the converter can generate. This leads to a decrease in the harmonic content and a better reconstruction of the sine wave that is generated by the power converter, as well as the reduction of the common-mode voltage [32].

Finally, the 32 possible phase voltages can be mapped into VSD variables by applying the Clarke transformation matrix (11), producing 32 voltage vectors represented in the α-β and x-y planes (z-axis component can be neglected in the star connection with isolated neutral point). Fig. 6 shows the projections of these vectors on each plane, where they have been numbered by the equivalent decimal number obtained from its corresponding switching state $\boldsymbol{S} = [S_a\ S_b\ S_c\ S_d\ S_e]^T$, being S_a and S_e the most and the least significant bits, respectively. It can be seen that there exist 2 null vectors and 30 active vectors, the last ones being classified in large ($0.647V_{dc}$), medium ($0.4V_{dc}$) and short ($0.247V_{dc}$) vectors. Thus, the space is divided in ten sectors of the same size with a separation of $\pi/5$ between them.

2.3. Experimental test bench

This illustrated review is based on a five-phase IM drive with distributed windings. Therefore, the contribution of the x-y plane to the electrical torque is neglected. Experimental results will be shown along the work to exemplify the performance of the system using different predictive current controllers. The experimental test bench depicted in Fig. 7 is used for this purpose. The test rig is composed by a three-phase IM rewound to have five phases with 30 slots and three pole pairs, whose electrical parameters are detailed in Table 1. The machine is supplied by two three-phase inverters from SEMIKRON that are connected to a DC-link voltage of 300 V from an independent DC power supply. The control algorithm is implemented in a TM320F28335 DSP placed on a MSK28335 Technosoft board. An external programmable load torque is also introduced in the system by means of an independently controlled DC motor. Finally, the rotor mechanical speed is measured using a GHM510296R/2500 encoder that is coupled to the shaft of the multiphase IM.

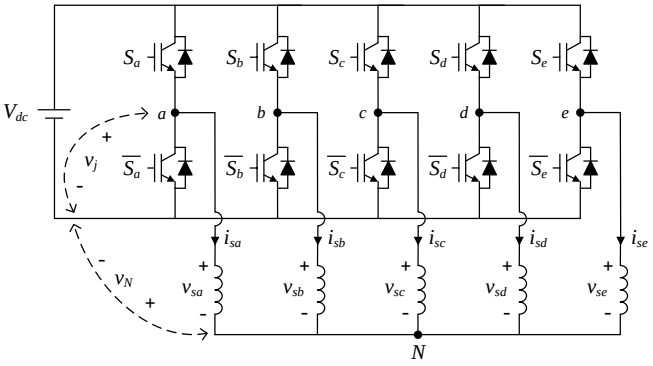

Fig. 5. *Scheme of the five-phase two-level VSI with star-connected load*

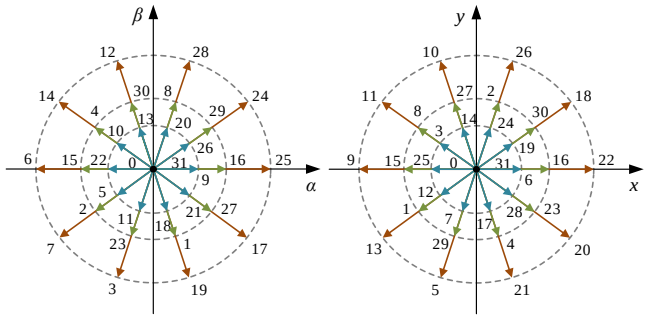

Fig. 6. *Space vector diagrams in the α-β and x-y subspaces*

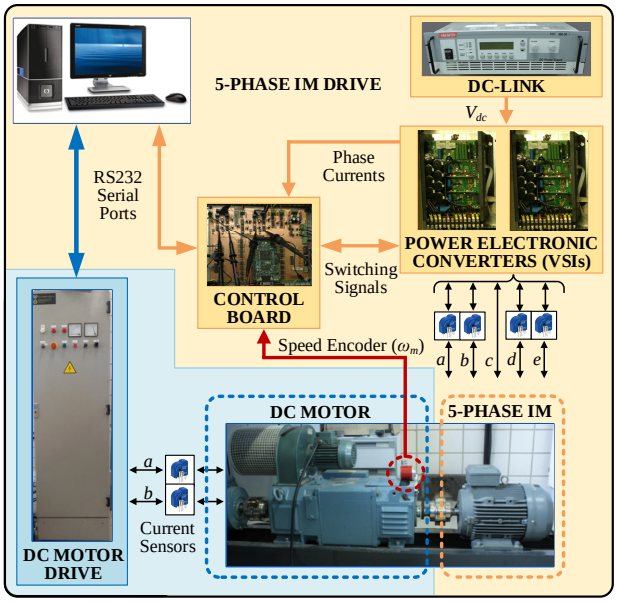

Fig. 7. *Graphic diagram of the experimental system*

Table 1. Electrical parameters of the machine

Parameter	Value
Stator resistance	19.45 Ω
Rotor resistance	6.77 Ω
Stator leakage inductance	100.7 mH
Rotor leakage inductance	38.6 mH
Mutual inductance	656.5 mH
Pole pairs	3
Stator rated current	2.5 A

3. Multiphase drives control techniques: the predictive current control approach

With the increasing interest in multiphase drives, the need for high-performance controllers has led the research activity in the last years. Conventionally, they are a complex extension of those applied

in the three-phase case, and their principal objective is the accurate and fast regulation of the speed and torque while fully exploiting the advantages of having more than three phases. The most widespread control technique applied to multiphase drives in the research literature and in industrial applications is the Vector Control (VC) or FOC. It is based on the use of Proportional-Integral (PI) regulators followed by a PWM stage that linearly provides the VSI switching combinations to be applied, hence it can be referred as a 'linear' controller. On the other hand, novel control strategies are appearing to simplify and enhance the multiphase control. These new techniques are based on 'non-linear' strategies, mostly known as 'direct' controllers, which do not include the PWM stage or other form of modulation. Conversely, they directly command the VSI forcing the controlled variables to rapidly follow their references. This is the case of the DTC method, which is the leading competitor of the FOC technique in three-phase drives; and the MPC technique, which has recently appeared as a promising alternative due to its flexibility and simple formulation. This section will be focused on the description of these methodologies and their most recent applications to multiphase drives, particularly to IM drives.

3.1. Field Oriented Control

The basis of the FOC technique, founded at the beginning of the 70s [33], is the independent control of the flux and torque of the AC machine in a similar way as it is done in a DC machine. For that purpose, a proper transformation of the controlled variables to the *d-q* plane is mandatory, where the *d*-axis is aligned with one of the flux components (air-gap, stator or rotor flux) in order to achieve the decoupling between flux and torque. Nowadays, the level of maturity of FOC for three-phase drives has permitted the total replacement of DC machines by AC ones in most industrial applications based on variable-speed drives.

In the case of multiphase drives, the higher number of degrees of freedom increases the complexity of the controller extension, as it is shown in numerous research works mainly based on the Indirect Rotor FOC (IRFOC) [11,34-38]. In this particular version of the control technique, the *d*-current is aligned with the rotor flux through the proper selection of the rotating reference frame angle in the Park transformation (θ in Fig. 4). In this way, the machine is fluxed by the *d*-current component while the electromagnetic torque is regulated by the *q*-component of the stator current. When applying the IRFOC to an IM, the orientation of the rotor flux in the required direction is done through the imposition of the slip speed in the following way:

$$\theta = \int_0^t (\omega_r + \omega_{sl})\, dt = \int_0^t \left(\omega_r + \frac{R_r\, i_{sq}^*}{L_r\, i_{sd}^*}\right) dt \qquad (35)$$

where reference values of the flux- and torque-producing stator currents (i_{sd}^* and i_{sq}^*) are normally used in the calculation process. However, a good knowledge of some machine parameters in the previous equation is necessary for a good orientation. Other versions of the FOC technique can be encountered in the literature with different flux components aligned with the *d*-axis and various estimation methods in the flux angle calculation [24,33,39].

The general IRFOC control scheme for a five-phase IM with distributed windings is shown in Fig. 8. It has the same cascaded structure used for three-phase drives, with an outer speed controller and an inner current controller per current component. Both current and speed controllers are typically PI regulators. With this configuration, the speed controller establishes the *q*-current reference while the *d*-current reference is set as constant. Conventionally, its nominal value is selected if the reference speed is below the synchronization speed of the machine, or regulated to deflux the machine if the speed goes beyond the synchronization point (field weakening region). The outputs of the current controllers are the reference voltages that must be applied to the machine in order to follow the current references. In this process, compensations terms, e_d and e_q, are added to take into account the coupling of the *d-q* stator voltages equations and compensate in a feedforward manner the cross-coupling effect. These terms are highly dependent on the machine parameters.

The difference of the control scheme with respect to the three-phase case is the incorporation of additional PI regulators for the *x-y* currents. It should be emphasized that, although these currents can be theoretically zeroed in distributed-winding machines impressing zero *x-y* stator voltage components, this might not be the case in a real application if stator windings present some degree of asymmetry and/or if the impact of the VSI dead-time is not negligible [28,35]. Consequently, it is advantageous to regulate *x-y* currents to be zero. For the case of IMs without isolated neutral point, it is also necessary to include an additional controller for the homopolar current. From this, it is stated that the complexity of the control scheme increases with the number of phases, being necessary to add a higher number of PI regulators that should be independently tuned.

Once the voltage references are given by the PI regulators in the *d-q* and *x-y* planes, they are transformed to phase variables using the inverse of the Park and Clarke transformations. After that, these phase voltages are modulated with some type of PWM strategy, conventionally Carrier-Based or Space Vector PWM (CBPWM and SVPWM, respectively) techniques, providing the switching pattern to be released to the VSI. Although these PWM techniques are well established in the three-phase case and the extension of the CBPWM to multiphase drives does not imply further complexity, the same does not apply to SVPWM, whose extension to the multiphase case has been recently investigated [10].

More recent research works in the field of FOC are centered on the full exploitation of the additional degrees of freedom in multiphase machines, like in the case of the torque enhancement through harmonic injection in concentrated-windings induction machines and in permanent magnet machines with different number

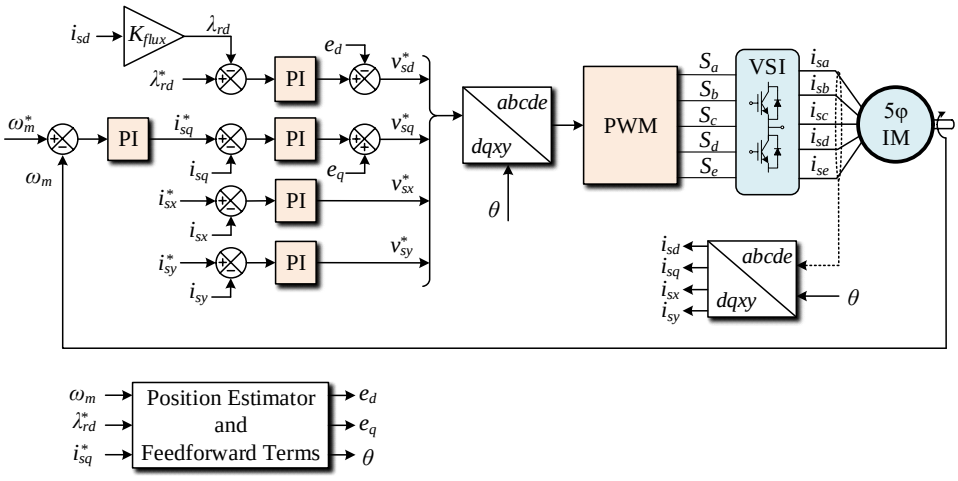

Fig. 8. *IRFOC technique for the distributed-windings five-phase IM drive*

of phases [40-44]. The extension of the FOC technique for the post-fault operation of the drive has also been addressed, focusing on the case of open-phase faults (the most analyzed post-fault situation in the literature [12]). A mandatory control reconfiguration is usually required to obtain the desirable fault tolerance [28,45-52], where three different actions have historically been necessary: *i*) estimation of new reference values of the *x-y* currents [28,50,51]; *ii*) reconfiguration of *x-y* controllers [45,50,52]; and *iii*) derating of the drive [45,47].

3.2. Direct Torque Control

Another well-established control technique in three-phase drives is the DTC, whose origin took place in the mid-80s [53,54]. Since then, numerous studies have been developed in the three-phase drives case [55], being the industrial implementation initiated by ABB [56]. The extension of DTC to different multiphase drives topologies has also been proposed [5,11], being nowadays a competitor to FOC due to its advantageous characteristics of robustness against machine parameters variation and fast flux and torque responses [57]. In its standard form, the controller maintains the outer PI speed controller as in FOC, but the inner current controllers are replaced by hysteresis blocks that directly regulate the fluctuations in the flux and the torque with respect to their references. In this case, the PI speed controller provides the torque reference (T_e^*) while the flux reference (λ_s^*) is again set constant or regulated to deflux the machine depending on the speed. Based on the output of these hysteresis blocks and an estimation of the flux position, the appropriate switching vector to be applied is selected through a predefined look-up table that takes into account all possible VSI states. The selected switching vector is directly released to the VSI without the intervention of a PWM stage. Continuing with the distributed-windings five-phase drive case example, the described scheme of the DTC is shown in Fig. 9.

As it can be seen, the control structure is simpler than in FOC, since Park transformation is no longer necessary, and the number of controlled variables is reduced to two, theoretically decreasing the computational cost. However, it presents important disadvantages, such as higher torque ripple and variable switching frequency, which depends on the operating point and the bandwidth of the hysteresis controllers. In addition, the control performance is highly dependent on the drive topology [58]. In order to mitigate these disadvantages, some modifications in the DTC structure have been proposed in the literature, such as the inclusion of PWM strategies [59,60] that leads to constant switching frequency and reduces the harmonic content, particularly on the *x-y* plane.

Most importantly, the extension of DTC to multiphase drives cannot completely regulate the *x-y* (and homopolar) currents with the basic control structure presented before, since only two variables (flux and torque) are controlled. As it occurs in FOC, these currents must be regulated to zero since they are only related to harmonic components and losses, except for the case of concentrated-windings machines. A recursive solution encountered in the literature is the definition of more elaborated look-up tables, or even the introduction of a second look-up table, in order to reduce the low-order harmonics and increase the efficiency [61-63]. Another solution just recently adopted is the use of virtual voltage vectors to nullify the average value of the *x-y* voltages and mitigate the *x-y* currents, while maintaining the original control scheme [30].

Most of the research works in the field of DTC are applied to five- and six-phase machines, but a recent work aims to extend the method to a higher number of phases [64,65]. Furthermore, the fault-tolerant capability of the DTC has been recently addressed for a five-phase IM drive. The study presented in [66] extends the DTC method used in normal operation of five-phase IM drives to the open-phase fault procedure. The post-fault DTC controller is similar to the scheme presented in Fig. 9 for healthy situation, but switching tables and applied virtual voltage vectors must be redefined after the fault occurrence to continue the operation of the multiphase drive. The performances of DTC and FOC controllers are compared in [67], where the advantages and disadvantages of these techniques in healthy and open-phase faulty situations are shown, introducing a powerful tool for the controller selection when using multiphase drives in final applications.

3.3. Model Predictive Control

A promising alternative to classical FOC and DTC methods, particularly in the multiphase drives field, is the model predictive control. This naming identifies a wide range of control techniques, whose functioning principle is based on the prediction of the future behavior of the system variables employing a mathematical model. The predictions are used to select the optimal control action to be applied according to a predefined cost function, which represents the control objectives [68]. The simplicity and intuitive formulation of the control problem has boosted the interest of the research community in the MPC strategy applied to electric drives [10,11]. Another reason has been the possibility to perform multi-objective and multi-variable control, or even to include non-linearities or constraints to the control process, just defining a proper cost function. This permits eliminating the classical cascaded structure in FOC, reducing the complexity of the controller and providing a fast dynamic response. Likewise, the high control flexibility of the MPC makes it a real alternative to DTC in the multiphase drive control area, since the main disadvantage of DTC is that it can manage the control of only two variables in its most conventional form.

However, MPC faces the important limitation of the high computational cost required to solve the optimization problem for all the control actions, which increases as the number of phases grows. For that reason, although the concept of MPC was developed in the 70s, its use has been traditionally restricted to systems with slow dynamics that permit performing the required calculations. This is the case of the petrochemical industry, which has constituted one of its main application fields during a long time [68,69].

Only with the recent development of fast and powerful microprocessors, the use of MPC in power converters and electric drives has become affordable [70]. Since then, the research activity in the field has given rise to numerous control approaches, being quite difficult to develop a general classification for all MPC techniques. Conventionally, they are divided in two wide categories: Finite-Control-Set MPC (FCS-MPC) and Continuous-Control-Set MPC (CCS-MPC) [71-73]. In both cases, the control principle is the

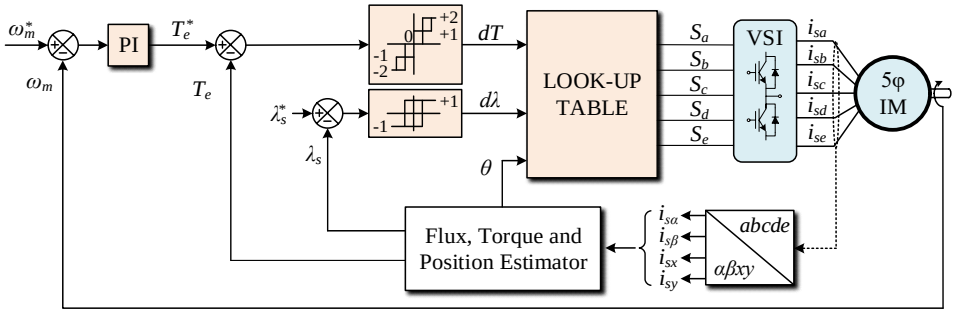

Fig. 9. *DTC technique for the distributed-windings five-phase IM drive*

same, i.e., a predictive model is used to calculate the optimal control action according to the control objective. The main differences between them rely on the type of mathematical model used for the predictions and how the control actions are applied to the system. In the FCS-MPC method, a discrete model of the system is used to compute the predictions and a predefined cost function determines the control objectives, usually composed by the errors between the predictions of the controlled variables and their references. Considering that the power converter supplying the machine presents a finite nature, with a limited number of possible switching states, FCS-MPC takes advantage of this situation and selects the optimal switching state that minimizes the cost function after an iterative process (optimization problem). The selected switching state of the power converter is then directly applied without any kind of modulator. On the other hand, a linearized or average model of the system is used in the CCS-MPC approach in order to provide continuous voltage references according to the control objective. Afterwards, the continuous voltages are modulated, conventionally by a PWM stage, providing the switching pattern to be applied to the power converter.

The differences between FCS-MPC and CCS-MPC schemes expose important advantages and disadvantages of both approaches. The inclusion of a modulator in the CCS-MPC allows for a linear formulation that permits avoiding the iterative process in the online optimization, thus requiring less intensive computation. Additionally, it fixes the switching frequency to a constant value, in contrast to the FCS-MPC where the switching frequency is variable. However, CCS-MPC offers a less flexible and more complex control scheme than FCS-MPC does, as a result of disregarding the discrete nature of the power converter. For that reason, most of the research activity in relation with MPC for multiphase drives is focused on the FCS-MPC technique. In this regard, the five-phase and six-phase machine topologies constitute the center of attention, both of induction or permanent magnet types [11,70,74], and the extension of the FCS-MPC to a higher number of phases is still difficult due to the exponential increase of the computational cost [75].

Independently of the predictive control structure, the most common application of MPC for multiphase drives is the result of its combination with a FOC technique. In this way, the outer speed control loop is maintained while the inner current regulators are substituted by an MPC current control. This control scheme is usually named Predictive Current Control (PCC) [76-80]. A comparative analysis between FOC and PCC techniques can be encountered in [79] and [80], where it is concluded that a better transient performance is obtained using predictive controllers. However, steady-state performance is superior with FOC, especially in terms of harmonic content in the controlled currents. Furthermore, the tuning of PCC requires less effort in contrast to FOC. As an alternative to the current regulation, the MPC scheme can be changed in order to control the flux and torque while maintaining the outer speed control loop. This scheme is named Predictive Torque Control (PTC) [81-85] and appears as a big competitor of DTC. This is demonstrated in [85], where the comparison between both techniques is performed and analyzed. Although DTC is less computationally demanding than PTC, the latter provides an extra flexibility for the regulation of non-torque/flux producing currents. As a result, the torque ripple is reduced in comparison with DTC, and faster torque and speed responses are observed. Further on, few proposals present an MPC approach in which both currents and speed are totally regulated with an MPC technique, and they are mostly referred to the three-phase case [86,87].

Focusing on the FCS-MPC technique using the PCC approach, the basic scheme is shown in Fig. 10, where the symmetrical five-phase IM fed by a two-level five-phase VSI is used again as case example. The FCS-MPC scheme is conventionally constituted by an outer speed control loop based on a FOC strategy, and an inner stator current control loop based on FCS-MPC. Notice that the described control scheme is formed by a fast inner current controller and an outer slower speed regulator that leads to a higher control bandwidth compared with the conventional cascaded structure of FOC [88].

The main objective of the FCS-MPC stator current controller is to determine, at every sampling time, the most adequate switching vector of the VSI ($\boldsymbol{S_{opt}}$) that must be applied in order to track the previously defined stator current references ($\boldsymbol{i_s^*}$). To this end, a discrete model of the system, commonly named predictive model, is used to predict the future behavior of the currents ($\boldsymbol{i_s^p}$) for a certain prediction horizon. These predictions are computed for all possible switching vectors (32 for the case of the five-phase IM drive) using the real values of the stator currents and the mechanical rotor speed ($\boldsymbol{i_s}$ and ω_m), which are measured through appropriate attached sensors. Then, the predictions are compared with their references in a cost function (J) that represents the control objectives. The minimization of the cost function provides the switching state that must be applied by the VSI during the entire sampling period. After that, a receding horizon strategy is applied and the whole process is repeated in the next sampling instant. The flow diagram of the described process is presented in Fig. 11.

The predictive model is obtained from the combination of the electrical equations of the IM expressed in terms of the VSD variables (15)-(16), and the VSI equation (34). The result is represented in state-space form, as it is shown in (36). The state vector is composed by the stator and rotor currents in the α-β-x-y reference frame $\boldsymbol{x} = \left[i_{s\alpha}\ i_{s\beta}\ i_{sx}\ i_{sy}\ i_{r\alpha}\ i_{r\beta}\right]^T$, the control action is the switching vector $\boldsymbol{S}$, the controlled variables are the stator currents $\boldsymbol{x_s} = \left[i_{s\alpha}\ i_{s\beta}\ i_{sx}\ i_{sy}\right]^T$, and matrices $\boldsymbol{A}$ and $\boldsymbol{B}$ depend on the electrical machine parameters and the present value of the rotor speed [77]. Notice that a similar formulation is obtained for any multiphase machine with a higher number of phases, with the difference of additional equations for the extra planes.

$$\frac{d\boldsymbol{x}}{dt}(t) = \boldsymbol{A}\boldsymbol{x}(t) + \boldsymbol{B}\boldsymbol{S}(t)$$

$$\boldsymbol{x_s}(t) = \boldsymbol{C}\boldsymbol{x}(t) \tag{36}$$

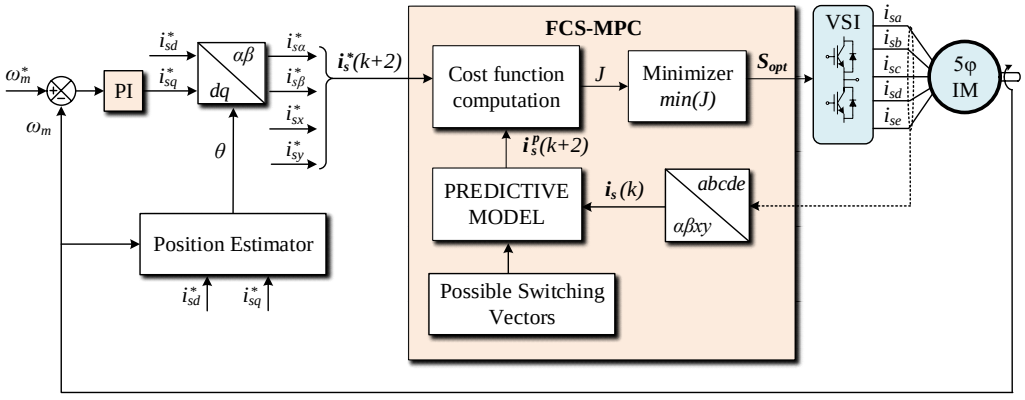

Fig. 10. *FCS-MPC technique for the distributed-windings five-phase IM drive*

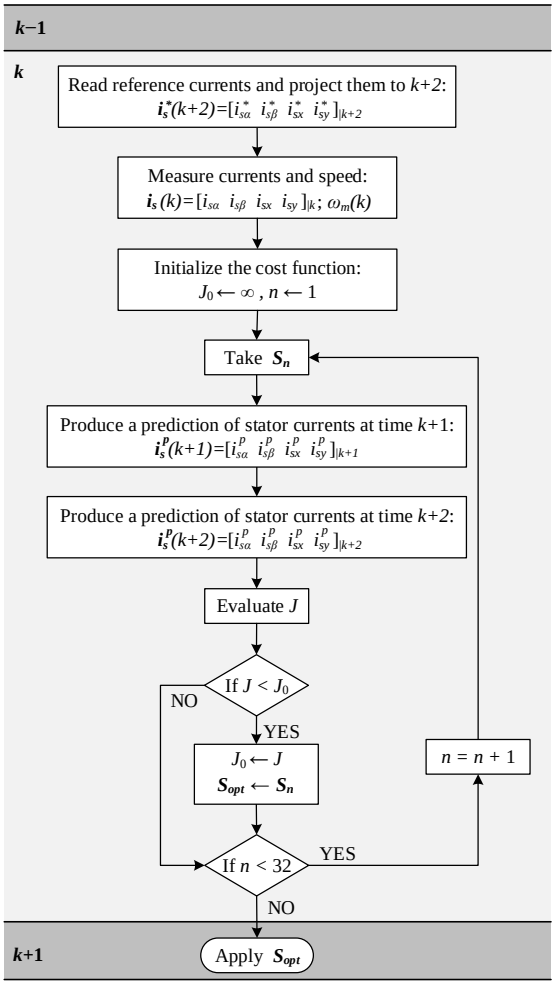

Fig. 11. *Flow diagram of the FCS-MPC technique*

Afterwards, this time-varying model is discretized in order to fit the discrete nature of the controller. For that purpose, an appropriate discretization technique is used. The forward Euler method is the choice of most FCS-MPC practitioners due to its simplicity, although different techniques can be used as it will be detailed in the next section. As a result, the general expression of the predictive model is the following:

$$\boldsymbol{x^p}(k+1) = \boldsymbol{x}(k) + T_s\big(\boldsymbol{A}\boldsymbol{x}(k) + \boldsymbol{B}\boldsymbol{S}(k)\big)$$

$$\boldsymbol{x_s^p}(k+1) = \boldsymbol{C}\boldsymbol{x^p}(k+1) \tag{37}$$

where T_s is the sampling time used in the discretization process and the superscript p indicates predicted values. Some FCS-MPC approaches replace the rotor currents by the rotor fluxes $\lambda_{r\alpha}$ and $\lambda_{r\beta}$ [89], or represent the system model in the *d-q* rotating reference frame [79]. In the latter case, the measured currents must also be rotated into the *d-q* plane after the application of the Clarke transformation. It is important to highlight the necessity to know the values of the rotor variables in order to compute the prediction of the stator currents. These variables cannot be usually measured in IMs, but they are estimated through the same predictive model using past values of stator and rotor currents [79]. Other conventional solution consists in gathering all unknown quantities of the system model and other uncertainties into one single term, thus constituting a new state variable. This new variable is tracked and updated at every sampling instant using, again, the system model and past measured values of the variables [77]. Considering the case under study, this technique leads to the new predictive model in (38), where $\boldsymbol{G^e}(k)$ is an estimation of the rotor currents contribution to the stator currents. This estimation is done holding the previous value $\boldsymbol{G^e}(k-1)$, which is computed at instant *k* applying (39). In these equations, $\overline{\boldsymbol{A}}$ and $\overline{\boldsymbol{B}}$ are sub-matrices derived from the original ones through simple mathematical calculations.

$$\boldsymbol{x_s^p}(k+1) = \boldsymbol{x_s}(k) + T_s\big(\overline{\boldsymbol{A}}\boldsymbol{x_s}(k) + \overline{\boldsymbol{B}}\boldsymbol{S}(k)\big) + \boldsymbol{G^e}(k) \tag{38}$$

$$\begin{aligned}\boldsymbol{G^e}(k) &= \boldsymbol{G^e}(k-1) = \\ &= \boldsymbol{x_s}(k) + \boldsymbol{x_s}(k-1) - T_s\big(\overline{\boldsymbol{A}}\boldsymbol{x_s}(k-1) + \overline{\boldsymbol{B}}\boldsymbol{S}(k-1)\big)\end{aligned} \tag{39}$$

Using either (37) or (38), the future values of the stator currents at instant *k+1* are computed using the measured values at instant *k* for each possible switching vector. The one that minimizes the control objective is selected and applied, ideally at instant *k*. However, the time required for the measurement, predictions calculation and selection of the optimal control action can be significant. Furthermore, this time is usually similar to the sampling time T_s, leading to an important delay between the instant when the measurements are done and the instant when the next control action is released. As a result, the selected control action is not applied at the correct moment producing a bad tracking of the references. This effect has been studied in the research literature [77,90] and can be corrected using different methods. The most common and simple one is the second-step ahead prediction that consists in computing predictions for *k+2* and applying the selected switching vector at *k+1* (see Fig. 11). Considering this, the predictive model is iterated two times and the cost function is defined for instant *k+2* as follows:

$$\begin{aligned}J = &\left(i_{s\alpha}^p(k+2) - i_{s\alpha}^*(k+2)\right)^2 \\ &+\left(i_{s\beta}^p(k+2) - i_{s\beta}^*(k+2)\right)^2 \\ &+K_{xy}\left(i_{sx}^p(k+2) - i_{sx}^*(k+2)\right)^2 \\ &+K_{xy}\left(i_{sy}^p(k+2) - i_{sy}^*(k+2)\right)^2\end{aligned} \tag{40}$$

As commented before, the cost function is conventionally constituted by the squared error between the stator current predictions and their references, and a common formulation in FCS-MPC current control of multiphase drives is the one presented in (40). Parameter K_{xy} is a weighting factor that permits to put more or less emphasis in the tracking of the *x-y* currents. However, different alternatives can be defined in order to include several control constraints and optimize the system performance. In that case, the definition of proper weighting factors for each control constraint is also possible. This flexibility is one of the main advantages of the FCS-MPC technique in comparison with classical control methods.

Stator current references are provided by the external FOC-based speed controller, being the IRFOC approach used in the case example, as shown in Fig. 10. Thus, a PI regulator provides the reference for the torque-producing current (i_{sq}^*), based on the difference between the measured speed and its reference. Conversely, the machine is fluxed by imposing a constant value of i_{sd}^* equal to the nominal one and the losses are minimized by setting null references for the *x-y* currents (note that it is assumed that the machine is working below the nominal speed and a defluxing regulation is not considered). Afterwards, the *d-q* stator current references are rotated into the *α-β* plane using the inverse of the Park transformation (21) and the estimation of the electrical angle θ (35). In order to be implemented in a microprocessor, equation (35) is discretized, usually applying a trapezoidal rule that uses past measured and estimated values at time instant *k*

$$\theta(k+1) = \theta(k) + T_s\big(\omega_{sl}(k) + P\omega_m(k)\big). \tag{41}$$

It is also interesting to highlight that the prediction horizon after the delay compensation is 2, so proper formulation of the rotating angle must be derived to estimate the future stator current references for instant *k+2*. This is possible assuming constant *d-q* current references for a sufficiently small sampling time [91].

To conclude this section, a comparison between FOC, DTC and FCS-MPC is illustrated in Table 2 and Fig. 12, where a qualitative

analysis is done based on the results presented in [67,79,85], supported with new experiments.

4. Key design and implementation features in FCS-MPC

The control system technology finds itself in a current paradigm-changing tipping point in which more demanding control goals, system flexibility and functionalities required by emerging applications are driving the control system development. In this context, FCS-MPC has proven to be a promising alternative in the control of multiphase drives. However, it is far from being mature yet, showing important limitations that require attention. Apart from the aforementioned problem of the high computational cost, there are additional drawbacks derived from the application of the FCS-MPC current controller:

- The high harmonic distortion that appears in the controlled currents as a direct consequence of the absence of a modulator and the fixed-time discretization nature of the control implementation. Note that standard FCS-MPC current controllers only apply a single switching state within a sampling period and, therefore, undesired *x-y* voltages are inevitably applied to the system as shown in Fig. 6.
- The high interdependence of the control performance with the predictive model. As a consequence, aspects not reflected in the predictive model act as disturbances that can deteriorate the system performance. This is the case of non-modeled effects, variations in the machine parameters, and non-measurable system variables, such as rotor quantities in the IM case.

Hereafter, some FCS-MPC implementation and design issues are commented, discussing as well some recent research approaches that improve the closed-loop operation and alleviate the aforementioned limitations.

4.1. Cost function design

In conventional FCS-MPC, the control goal is the tracking of the controlled variables according to their references. Thus, the cost function is formed by the difference between the predicted values of the controlled variables and their references, using an absolute or a quadratic norm for the error evaluation [70]. Both norms provide similar results in terms of tracking when only one error term is

Table 2. Qualitative comparison between FOC, DTC and MPC techniques [67,79,85].

System performance	FOC	DTC	MPC
Outer controller	PI	PI	PI
Inner controllers	PI	Hysteresis	Cost function
Modulation stage	Yes	No	No
Switching frequency	Fixed	Variable	Variable
Control of the secondary plane currents	Additional pair of PI controllers	Open-loop control	Current error in the single cost function
Dependence of parameters	Yes (rotor position estimation)	Yes (stator flux estimation)	Yes (model of the machine)
Computational cost (using TM320F28335 DSP)	$\sim 30\mu s$	$\sim 20\mu s$	$\sim 50\mu s$
Tuning/retuning for different operating points	Difficult, retuning required	Easy, retuning not required	Easy, retuning not required
Stator current THD	Low	Very high	High
Transient response	Slow	Fast	Fast

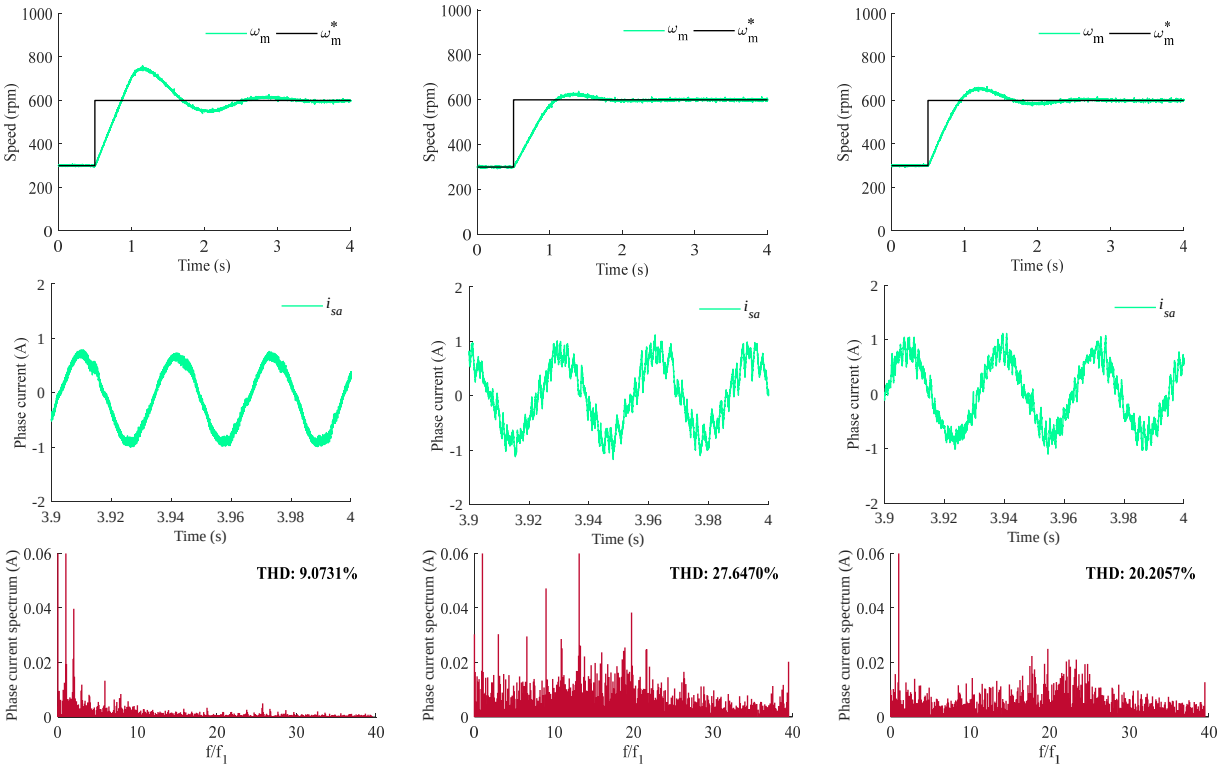

Fig. 12. *Speed step response, using the test rig of the five-phase IM drive presented in Fig. 7 and Table 1, for FOC (left plots), DTC (middle plots) and FCS-MPC (right plots). The applied control parameters are those used in [67]. From top to bottom: speed response, phase current i_{sa} and zoomed harmonic spectrum of phase currents*

considered in the cost function, but the quadratic error is preferable when several error terms are evaluated [91], so it constitutes the usual selection in multiphase drives. For instance, in FCS-MPC current control the cost function only depends on the squared current error, as it was shown in (40) for the case of the five-phase IM drive. Conversely, when an FCS-MPC torque control is implemented, the cost function is constituted by the error in the flux and torque tracking as follows:

$$J = \left(T_e^p(k+2) - T_e^*(k+2)\right)^2 + K_\lambda\left(\left|\boldsymbol{\lambda}_s^p(k+2)\right| - \left|\boldsymbol{\lambda}_s^*(k+2)\right|\right)^2. \quad (42)$$

Regardless of the controlled variables, it is a common practice to include weighting factors (K_{xy}, K_λ) when several terms are considered in the control objective, especially when they are of different nature. This permits adjusting the importance of each controlled variable. Additionally, the cost function provides high flexibility to include additional terms that represent supplementary control objectives, as it was previously commented. Consequently, it is possible to improve several control aspects just modifying the cost function [73]. Concerning multiphase drives, several examples can be encountered in the literature. In [89], the cost function is designed in order to additionally reduce the common-mode voltage in the FCS-MPC current control of a five-phase IM drive. The reduction or limitation of the switching frequency in the power converter (VSI losses) has also been studied in [83] for the torque control of a PMSM, and in [92] for the current control of a five-phase IM. This is achieved by restricting the number of switching operations of the power switches at each sampling period. Another non-conventional control objective, barely applied to multiphase drives, is the reduction of the harmonic content in the controlled variables through the imposition of specific pulse patterns in the VSI or by the selective harmonic elimination. These techniques, particularly the last one, can require complex formulations and calculations, being its application principally restricted to particular topologies of power converters [72,93-95].

Further on, the flexibility of the FCS-MPC technique permits the inclusion of non-linearities or constraints in the cost function, this being more complicated to achieve using linear controllers. This is usually done by adding non-linear terms in the cost function (e.g., logic functions), which are multiplied by larger weighting factors. Thus, the control actions that do not comply with the restrictions are discarded during the optimization problem. Some examples can be found in [80,84,95] for the FCS-MPC torque control of multiphase drives, where the stator currents are limited to a maximum value in order to avoid over-current situations during transients.

In all previously described cases, the use of weighting factors is common. However, the performance of the controller can drastically change depending on the selected values of these weighting factors. Consequently, it is necessary to properly tune these parameters for the considered application and control requirements. This is usually done through trial and error experiments [96], or using more complex optimization algorithms [73,91,97]. In any case, the optimal selection is based on some established figures of merit, such as current tracking error, harmonic content or switching losses. For example, the weighting factors can be configured in order to provide a good current tracking performance while maintaining reduced switching losses [91]. However, the tuning of the weighting factors is not an easy task in some cases, since the optimal value can vary depending on the considered operating point, among other causes. As an example, in [78] the FCS-MPC current control of a five-phase IM is studied using the cost function in (40), where different sets of possible switching vectors are considered in the optimization process. This study concludes that the value of K_{xy} that provides a good trade-off between the current control in the primary and secondary planes can be quite different depending on the considered set of switching states and the operating point. A deeper analysis of the situation is performed in a recent research work [98], where it is stated that some of the figures of merit conventionally used in the tuning process are not independent (e.g., the harmonic content is directly related with the switching frequency). Consequently, there exist fundamental trade-offs that cannot be overcome just by the cost function design. A summary of this analysis is presented in Table 3, showing the values of the average switching frequency and the Root Mean Squared (RMS) tracking error in the α-β and x-y subspaces, for different values of K_{xy}.

4.2. Predictive model design

The predictive model constitutes another key element in the performance of any MPC controller, since the selected control actions during the optimization problem depend on it. This implies that the more accurate the designed predictive model is, the more precise the predictions are and, consequently, the performance of the control system improves. Direct consequences of inaccurate predictions can be the increment in the steady-state tracking error or in the harmonic content of the controlled variables. However, the degree of complexity of the predictive model must guarantee a compromise between accuracy and computational burden.

In this regard, important aspects must be discussed, being the first one the discretization technique used in the design process of the predictive model. Although there exist several alternatives, the first-order forward Euler approximation is usually enough to obtain an accurate discrete model of a system, thus constituting the most widespread election for multiphase drives. It was previously seen that the application of the forward Euler discretization provides the predictive model in (37) for the five-phase IM case. This is a simple formulation that requires easy calculations, only being necessary to update every sampling period the matrices coefficients related to the rotor speed. However, there are special situations when an alternative strategy is required, as it is the case when the sampling frequency is too low or when there exist high pass filters in the plant. In these cases, a bilinear discretization or the so-called 'exact discretization' is more convenient. In the last years, the use of the exact discretization has appeared in some research works in relation with the FCS-MPC control of multiphase drives [68,89,100]. The triggering factor was the work in [81], where it was stated that the discretization technique based on the Cayley-Hamilton theorem provides better tracking and prediction performances than conventional Euler methods. Continuing with the five-phase IM drive example, the discretization of the system equations using this method leads to the following predictive model:

$$\boldsymbol{x}^{\boldsymbol{p}}(k+1) = \boldsymbol{\Phi}\boldsymbol{x}(k) + \boldsymbol{\Gamma}\boldsymbol{S}(k)$$

$$\boldsymbol{x}_{\boldsymbol{s}}^{\boldsymbol{p}}(k+1) = \boldsymbol{C}\boldsymbol{x}^{\boldsymbol{p}}(k+1) \quad (43)$$

Table 3. Values of the figures of merit obtained in [99] for several choices of the parameter K_{xy}

K_{xy}	RMS tracking error in α-β subspace (A)	RMS tracking error in x-y subspace (A)	Average switching frequency (Hz)
0.005	0.102	0.394	5950
0.050	0.144	0.228	4820
0.500	0.153	0.174	4591
1.000	0.168	0.159	4423
3.000	0.193	0.154	3991
7.000	0.249	0.143	3670

where the new matrices are $\boldsymbol{\Phi} = e^{\boldsymbol{A}T_s}$ and $\boldsymbol{\Gamma} = \int_0^{T_s} e^{\boldsymbol{A}t}\boldsymbol{B}dt$. Since matrix $\boldsymbol{A}$ depends on the instantaneous value of the rotor speed, the computation of these matrices is not straightforward and requires complex calculations. This constitutes the main disadvantage of this discretization technique compared to Euler approaches. Nonetheless, it is possible to simplify the calculations to some extent using the Cayley-Hamilton theorem and assuming that the mechanical dynamics are slow enough during a sampling period to consider the rotor speed constant, as it is described in [81] and [101].

Another important aspect related to the predictive model is its high dependence on the system parameters. For the case of electric drives, the electrical parameters of the machine are commonly estimated using offline methods, such as the ones described in [25,26,102], and it is assumed a good agreement with the reality during the whole system operation. However, this is far from being a real assumption, since these parameters may not be precisely estimated and usually their values vary during operation due to thermal, saturation or deep-bar effects, which are not considered during the offline parameter estimation process. Consequently, the parameter uncertainty can lead to inaccurate predictions, deteriorating the performance and stability of the predictive algorithm. This issue has been recently investigated in the literature, being the conventional three-phase power converters and permanent magnet drives the main focus [103-107]. In general, it is seen that errors in the inductances of the system are usually related to current ripple, while variations in resistances or flux linkages (in the case of permanent magnet machines) mostly affect the steady-state errors and dynamic response.

Conversely, the sensitivity to parameters in the field of multiphase drives, where more electrical variables must be taken into account due to the higher number of degrees of freedom, has been barely investigated and only two significant sensitivity analyses can be encountered for a five-phase IM drive [100,108]. Particularly, experimental results are conducted in [100] for a wide range of operating conditions and machine parameters detuning situations. The obtained conclusions reveal that the FCS-MPC performance in terms of phase-current tracking is principally altered by the detuning of the mutual inductance (L_m) and the rotor resistance (R_r). Furthermore, this effect is boosted by changes in the operating point. On the contrary, stator leakage inductance (L_{ls}) hardly affects the performance, and the impact of the stator resistance (R_s) and the rotor leakage inductance (L_{lr}) is negligible. A deeper analysis reports that the current control performance in the *d-q* and *x-y* planes is also principally influenced by the variations in L_m and R_r. Therefore, inferior flux and torque regulation with higher harmonic content and copper losses are reported when large variations are introduced in these parameters. In this concern, the *d-q* current tracking performance is slightly altered by the detuning of L_{ls} and R_s, while the electrical noise content in the *x-y* currents is not much influenced by changes on L_{ls}. It is important to highlight that disturbances in the speed response are not reported in any experimental test for the considered ranges of parameter detuning. A summary of the described conclusions are presented in Table 4, where symbol '$-$' indicates negligible impact.

Several online techniques have also been proposed in the literature to cope with the parameter mismatch, as well as with other uncertainties and non-modeled effects that can compromise the performance of the predictive controller. The main objective is to provide robustness and stability to the predictive controller against these disturbances. Some proposals are based on online parameter identification algorithms [106,109], but the major interest is given to the use of adaptive and disturbance observers [96,104,110-113]. The observer theory permits the estimation of not only parameter deviations, but also other unknown system variables, such as rotor fluxes, rotor position or speed (in the case of sensorless control). With these methods, an online estimation of modeling uncertainties is performed inside the control algorithm, conventionally using the same mathematical system models and measured information that are employed for the prediction calculations. However, these models are slightly modified in the case of the observer technique, where some correction terms are added. This implies that the observers will require a tuning process in most cases. As a result of the computation of the uncertainties estimations, the system performance in terms of harmonic content, torque ripple and switching losses is generally improved. It must be highlighted that most applications of the observer theory are related to conventional three-phase machines, particularly the PMSM topology. Only recently, its extension to the multiphase case has been developed in [114-117], where observers based on Luenberger and Kalman filters have been used for the rotor current estimation in FCS-MPC current control of five-phase IM drives. The obtained results validate the effectiveness of the rotor current observers (see Table 5), improving the predictions and the current control performance, at the expense of slightly increasing the complexity of the controller and the computational cost.

4.3. Implementation of the control algorithm

The FCS-MPC suffers from a considerable computational cost, particularly when it is applied to multiphase drives. To illustrate this issue, a particular real-time implementation of the FCS-MPC technique in a TMS320F28335 microprocessor is shown in Fig. 13. This graphic reveals the time-consuming computing load (in μs) of every implemented task during a sampling period, using the FCS-MPC current control of the five-phase IM drive as a case example. It can be seen that the FCS-MPC current controller (i.e., prediction of stator currents, optimization of the cost function and application of the selected switching voltage vector) constitutes the most time-demanding task with 36 μs, followed by the A/D conversion process of all measurements (8 μs). Meanwhile, the IRFOC-based speed controller and other processes (including data logging for external analysis and PC-DSP communication) are not heavy from the computational cost perspective (2 and 4 μs, respectively).

In order to alleviate this problem, it is possible to consider a reduced set of switching states in the optimization algorithm of the FCS-MPC. This approach has been tested in [76,77] for a six-phase IM drive, reducing the number of voltage vectors from 64 to 49 and 13. However, suboptimal solutions are obtained since not all possible control actions are considered, and this can be detrimental to other control performance aspects. Another proposal based on the previous ones is presented in [118]. Its basic functioning is the application of an algorithm, at every sampling time and before the optimization problem computation, in order to find a subgroup of possible switching vectors that comply with some conditions. These conditions look for the limitation of the power switching operations, so this technique also provides lower average switching frequencies compared to conventional FCS-MPC approaches. A more recent alternative in [119] proposes the selection of a subgroup of voltage vectors based on the instantaneous flux position and the torque deviation in the *α-β-x-y* axes for the PTC control of a PMSM. The

Table 4. Qualitative results of the sensitivity analysis to parameter variation performed in [100] for the FCS-MPC current control of a five-phase IM drive.

Impact on the system performance	L_m	R_r	L_{ls}	R_s	L_{lr}
Speed performance	–	–	–	–	–
Phase current RMS error	↑↑↑	↑↑↑	↑	–	–
d-q current performance	↑↑↑	↑↑↑	↑↑	↑	–
x-y current performance	↑↑↑	↑↑↑	↑	–	–

Table 5. Results obtained in [117] for different stator current references defined by a frequency f_e and an amplitude A_{ref}, using three different FCS-MPC controllers: without rotor current observers, with reduced-order rotor current observer (RLO) and with full-order rotor current observer (FLO).

Control technique	RMS tracking error in α component (A)	RMS tracking error in x-y components (A)	RMS prediction error in α component (A)	Total harmonic distortion (%)
		f_e = 19 Hz, A_{ref} = 1.47 A		
FCS-MPC	0.1071	0.1774	0.1438	10.15
FCS-MPC + RLO	0.0893	0.1336	0.1030	10.36
FCS-MPC + FLO	0.0732	0.0885	0.0780	8.56
		f_e = 24 Hz, A_{ref} = 1.50 A		
FCS-MPC	0.1096	0.1775	0.1425	8.69
FCS-MPC + RLO	0.0836	0.1309	0.1017	7.95
FCS-MPC + FLO	0.0712	0.0841	0.0834	6.46
		f_e = 29 Hz, A_{ref} = 1.62 A		
FCS-MPC	0.1091	0.1844	0.1507	7.09
FCS-MPC + RLO	0.0784	0.1434	0.1031	6.96
FCS-MPC + FLO	0.0661	0.0828	0.0893	5.22
		f_e = 34 Hz, A_{ref} = 1.56 A		
FCS-MPC	0.1123	0.1889	0.1541	7.24
FCS-MPC + RLO	0.0782	0.1538	0.1042	6.63
FCS-MPC + FLO	0.0612	0.0827	0.0927	5.10
		f_e = 39 Hz, A_{ref} = 1.60 A		
FCS-MPC	0.1212	0.2176	0.1602	6.39
FCS-MPC + RLO	0.0782	0.1817	0.1068	5.70
FCS-MPC + FLO	0.0610	0.1274	0.1040	4.46

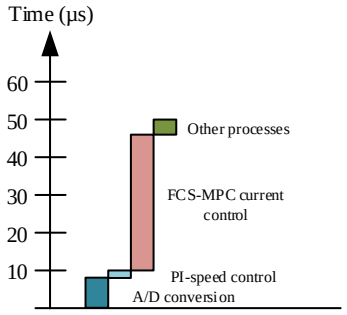

Fig. 13. *Time-consuming computing load (in µs) of every implemented task during a sampling period, using the FCS-MPC current control applied to the five-phase IM drive*

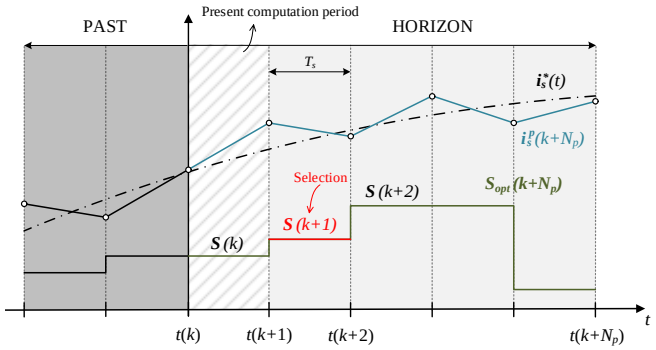

Fig. 14. *Schematic representation of the optimal switching vector selection in the FCS-MPC with prediction horizon N_p*

imposed conditions principally try to reduce the harmonic and flux content in the x-y subspace. It is however remarkable that, in all cited techniques, a group of possible control actions are discarded, and the potential of using all available voltage vectors is not fully exploited in the compliance of the main control objectives.

Concerning the FCS-MPC steady-state response, interesting alternatives to the conventional control algorithm can be found in the literature with the aim of improving the system performance. One of them is the use of an extended prediction horizon [120], defined as the number of future time instants in which the controlled variables will be predicted in order to select the optimal control action. There exist different variations of this technique in its application to power converters and electric drives [121]. As an example, consider the case when the switching horizon equals 1 ($N_s = 1$) and the prediction horizon is equal or superior to 2 ($N_p \geq 2$). The optimization algorithm has to find the optimal sequence of switching vectors $\boldsymbol{S_{opt}} = [\boldsymbol{S}(k+1)\,\boldsymbol{S}(k+2)\,...\,\boldsymbol{S}(k+N_p)]$ that must be applied to the power converter in order to follow the imposed reference in the whole considered prediction horizon. Thus, predictions must be computed for all possible switching vectors and all time instants covered by the prediction horizon. In other words, the number of computed predictions reaches $(N_p - 1)2^n$, being n the number of phases in the converter. Afterwards, only the first switching vector in the selected sequence is applied at the next sampling instant (the process is illustrated in Fig. 14). Although it has been demonstrated that long prediction horizons can improve the performance, particularly in relation to the harmonic content and steady-state error, the computational burden can be enormous. For this reason, advanced optimization algorithms are usually applied, such as move-blocking and extrapolation strategies, with a compromise between performance improvement and computational cost [121]. However, there are still cases when the high calculation time due to long prediction horizons is hardly affordable at a reasonable cost with the computing capability of modern electronic devices and microprocessors. This is the case of multiphase drives.

Different approaches can be encountered with the more specific objective of reducing the harmonic content in the controlled variables. As previously stated, the main origin of this problem is the fixed-sampling nature of the FCS-MPC algorithm combined with the absence of a modulator. Although only one switching vector is applied in a sampling period, it can be maintained during several periods, hence its total application time depends on the imposed sampling time. This has a high impact on the harmonic content of the currents, as it has been recently studied in [122], leading to a spread spectrum with a significant amount of harmonics and electrical noise. Some recent research works mitigate this problem applying two or more switching vectors during the same sampling period, which can be seen as a kind of modulation process. For example, in [123] a combination of a zero and an active vector is applied every sampling instant, being the active vector selected following the same optimization problem than the one employed in the conventional FCS-MPC scheme. Then, the application time of the active vector is computed using a linearized and reduced order

model that depends on predicted, measured and reference values of the controlled variables. Similar approaches can be found in [124,125], where proper PWM methods are applied and a fixed switching frequency is guaranteed. Finally, another strategy consists in the use of virtual voltage vectors in an MPC method (VV-MPC) instead of the conventional VSI switching vectors, in a similar way as it is done in DTC [126-128]. The obtained results have revealed the enhancement in the system efficiency by reducing the harmonic content, mainly in the *x-y* plane. Moreover, this technique presents a lower computational cost since reduced predicted models and cost functions are employed, even though it tends to provide higher switching frequencies than the conventional approach in some cases and reduces the available voltage limits.

5. Future prospects in the MPC field

In the humble opinion of the authors, there are some recent research works in the application of MPC techniques to multiphase drives that go beyond the described control goals or try to alleviate aforementioned difficulties and seem to be interesting for future research. In particular, three main areas attract authors' attention.

The first one is in relation to the inclusion of electrical limits in the control strategy of the multiphase drive. Optimal control techniques have appeared as a viable candidate to this end in classical three-phase drives [129], and many algorithms have been so far proposed in the scientific literature based on this industrial requirement [130]. For instance, the switching frequency and the current control limits are considered in [131] to avoid an excessive temperature increment in the critical components of the system. Optimal *d-q* current control vectors are estimated to maximize the drive efficiency and the speed-torque performance within the temperature and voltage constraints. The reference flux is also evaluated to guarantee the maximum torque capability over the entire speed range of induction [132-135] or permanent magnet [136] machines. More recently, different optimal controllers have been presented and experimentally compared in [137], where PMSM drives are again considered. Most of these scientific studies, if not all, focus on conventional three-phase drives, where one *d-q* reference subspace appears and an analytical expression of the optimal reference stator currents that respects the imposed constraints can be easily obtained. Indeed, the machine flux is usually weakened (the *d*-current component is reduced) to respect the imposed voltage limit, adjusting at the same time the *q*-current component with the aim of complying with the current limits. However, the situation becomes much more complex when a multiphase electromechanical drive is considered. Optimal controllers can enhance the benefits of using multiphase machines, but the appearance of multiple orthogonal *d-q* control subspaces involved in the torque production of the multiphase drive highly complicates the extraction of the maximum torque under electrical limits and constraints. The problem of applying an optimal controller in a multiphase drive is in relation with the difficulty to obtain analytical expressions for the electrical references in the orthogonal *d-q* sets from the electrical phase limits, where a dependency appears. In general terms, the peak value of the phase voltage (current) depends on the voltages (currents) in each *d-q* subspace, which are unrelated and have different frequencies, magnitudes and phase shifts. This dependency has recently been simplified using offline assumptions to force an analytical relation between the electrical references in the orthogonal *d-q* subspaces, obtaining a kind of suboptimal controller. This is the case in [42,138], where the worst-case scenario is considered, assuming that all *d-q* voltage (current) components reach their peak values at the same time instant. This gives in fact safety performance margins in the system, but the obtained results cannot be considered as optimal. An interesting alternative based on offline look-up tables appears in [139]. In this case, *d-q* reference currents are generated using a preliminary minimization technique that finds the minimum of a constrained nonlinear multivariable function. These values are then placed in reference tables to be used in the control strategy. A significant consequence is that steady-state reference values are found and used in look-up tables, and the defined controller has the ability to manage failure mechanisms and critical electrical limits.

A potential alternative for the definition of optimal regulators can be the use of MPC techniques for solving the optimization and control problems. It is noteworthy that MPC techniques have been widely used to solve control problems in electrical applications with power converters, giving a high flexibility and including different control objectives and/or constraints, as stated along this work. However, electrical limits for multiphase drives have been first considered in [140,141] using a two-stage predictive controller (see Fig. 15). Firstly, a CCS-MPC stage produces optimal reference currents, taking into account programmed electrical and magnetic constraints. Secondly, an FCS-MPC controller regulates the stator currents of the system in order to track the optimal references. Therefore, optimal current controllers using MPC techniques are introduced, which allows the optimal utilization of the system torque capability under voltage, current and magnetic limitations. The obtained results should encourage the scientific community to work in this field, to overcome the obtained limitations, mostly in relation with the online implementation of the controller and the applied optimization algorithm.

The second future prospect focuses on the use of predictive controllers with variable sampling time. Predictive controllers and multiphase drives have been developed hand in hand and most common findings show that the computational cost of the controller is a serious handicap for its implementation, and that high harmonic content is generated due to the fixed sampling-time nature and the absence of modulation methods in the control algorithm. Regarding the harmonic content, different methods have explored the possibility to reduce it, as in the case of including rotor current observers to create a more precise predictive model of the multiphase machine. However, a more natural way to face the harmonic problem consists in introducing the concept of non-uniform sampling time as a new degree of freedom in the FCS-MPC technique. The idea was firstly exposed in [143] for a three-phase IM drive, but it has been further developed and extended to the five-phase case in recent works [143-145], where the lead-pursuit concept is incorporated reducing the complexity of the controller with respect to the original approach. The proposed control structure, named Variable Sampling Time Lead Pursuit Control (VSTLPC), is divided in two steps (see Fig. 16). Firstly, the lead-pursuit concept is applied to select the optimal VSI state ($\boldsymbol{S_a}$) based on predefined stator current references. Secondly, its time of application (T_a) is calculated using the space-state model of the system and predicting the future behavior of the controlled currents. An observer is also incorporated to estimate the rotor currents thus improving the predictions. The results of these publications validate the effectiveness of the proposal, particularly to reduce the current harmonic content and to improve the current tracking performance when compared to the conventional FCS-MPC approach, as it can be seen in Fig. 17. This is, in essence, a completely new technique that has been only tested using a five-phase IM with symmetrical and distributed windings as a case example. Then, it is expected much more work in the field in the recent future.

Finally, among the different possibilities to exploit the additional degrees of freedom in multiphase drives, the fault tolerance has been an interesting research subject in recent times. This inherent capability is highly appreciated, but it typically requires fault detection and localization of the fault in a first stage [146-148], and the reconfiguration of the control scheme in a second one. The standard techniques in normal operation have been modified to become fault-tolerant: IRFOC [28,45-52], DTC [66] and MPC [149,150]. Moreover, the performances of these three controllers are compared in [67] when an open-phase fault appears in a five-phase IM drive, concluding that there is no ideal controller to manage the fault situation (see Table 6). In such controllers, the reconfiguration stage involves the use of different Clarke transformations, cost functions and current references for each of the multiple open-phase

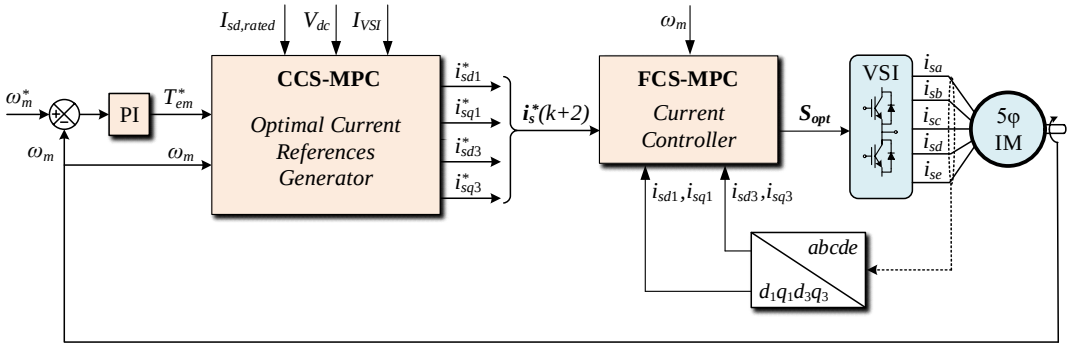

Fig. 15. *Predictive controller scheme considering electrical constraints in the control strategy*

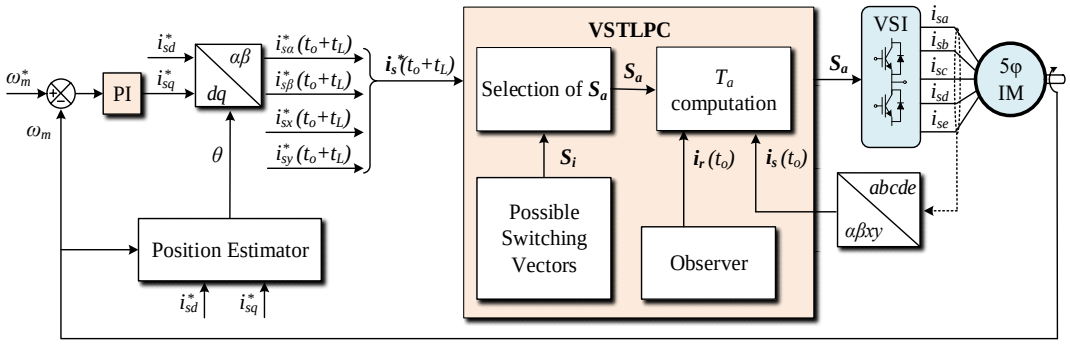

Fig. 16. *VSTLPC technique for the distributed-windings five-phase IM drive*

Table 6. Qualitative comparison between IRFOC, DTC and MPC methods in open-phase fault operation.

Closed-loop system performance	IRFOC	DTC	MPC
Speed tracking error when the fault appears	Negligible	Slight	High
Torque tracking loss during a detection delay	Yes	No	Yes
Robustness against fault detection delay	↓	↑↑	↓↓
Change in the Clarke transformation	No	Yes	Yes
Computational cost	↑	↓	↑↑
Stator current THD	↓	↑↑	↑
Maximum available torque	56% of T_n	50% of T_n	56% of T_n

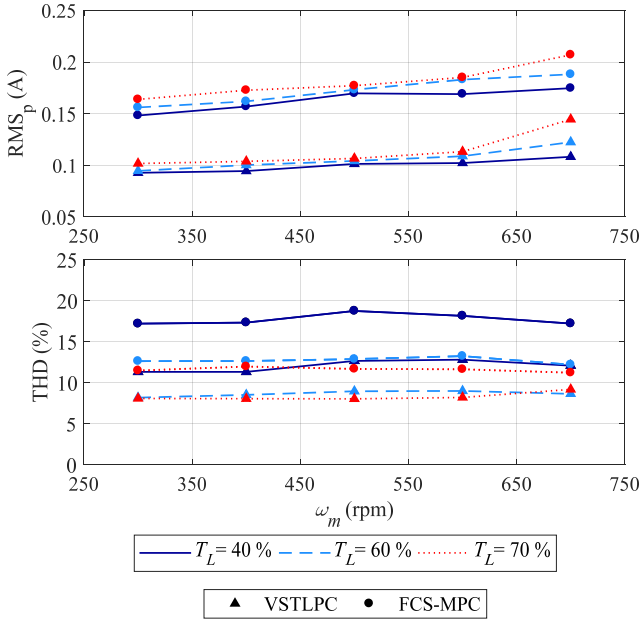

Fig. 17. *Experimental RMS error (RMS_p) and total harmonic distortion (THD) of the phase stator currents for different speeds (ω_m) and load torques (T_L) presented in [143], when applying the VSTLPC and conventional FCS-MPC techniques to the distributed-windings five-phase IM drive*

fault scenarios. However, a recent study presented in [151] proposes the implementation of the VV-MPC strategy of [126] for the fault operation, allowing to conduct the control of the *x-y* currents in open-loop mode. This fact provides FCS-MPC with a natural fault tolerance (a ripple-free post-fault performance without mandatory control reconfiguration), since the conflict between *α-β* and *x-y* current controllers is avoided. This, in practice, provides a smoother transient from healthy to faulty operation and makes the control immune to fault detection errors or delays, opening up a new avenue of study in the topic [151,152].

6. Conclusion

Some recent review papers have been published both in the field of multiphase drives and in the area of predictive controllers applied to power electronics. Nevertheless, the covered research content in these works was so vast that the simultaneous analysis of multiphase drives and predictive controllers as a common research field was not possible. Even though this joint field could be initially considered as a subtopic in the study of multiphase drives, the ever-increasing interest in the last decade suggests considering it as a new research area. The number of papers dealing with predictive controllers in multiphase systems has reached a critical mass, and for that reason this work presents a detailed and updated state-of-the-art review of this area. Furthermore, the aim is not only to review the existing works, but to provide a framework of analysis and guidelines for the implementation of predictive controllers to regulate multiphase drives. For this purpose, this paper takes the five-phase case to clearly illustrate the different issues that should be mandatorily considered by researchers and practitioners that are willing to

achieve a successful predictive control of multiphase machines. Lastly, this work also points out three fields that are identified as future research trends with a significant potential for contribution: the inclusion of electrical limits in the control of multiphase drives, the use of predictive controllers with variable sampling time and the design of robust multiphase drives with a natural fault-tolerant capability. The whole work is conceived not only to present the recent research to the scientific community, but also to introduce the field to new researchers and practitioners in order to promote future research and engineering applications.

7. Acknowledgments

The authors would like to thank Prof. Emil Levi, from the Liverpool John Moores University (UK) for his support in the multiphase drives research field. This work would not have been possible without his selfless help, knowledge, tips and supervision during the last 15 years.

8. References

[1] Amsterdam Roundtables Foundation and McKinsey & Company: 'Electric vehicles in Europe: Gearing up for a new phase?', available online: https://www.mckinsey.com/featured-insights/europe/electric-vehicles-in-europe-gearing-up-for-a-new-phase, 2014.

[2] Warg, E.E., Härer, H.: 'Preliminary investigation of an inventor-fed 5-phase induction motor', *Proceedings of the Institution of Electrical Engineers*, 1969, **116**, (6), pp. 980–984

[3] Jahns, T.M.: 'Improved reliability in solid-state AC drives by means of multiple independent phase drive units', *IEEE Transactions on Industry Applications*, 1980, **IA-16**, pp. 321–331

[4] Toliyat, H.A., Lipo, T.A., White, J.C.: 'Analysis of a concentrated winding induction machine for adjustable speed drive applications. I. Motor analysis', *IEEE Transactions on Energy Conversion*, 1991, **6**, (4), pp. 679–683

[5] Levi, E., Bojoi, R., Profumo, F., Toliyat, H.A., Williamson, S.: 'Multiphase induction motor drives – a technology status review', *IET Electric Power Applications*, 2007, **1**, (4), pp. 489–516

[6] Levi, E.: 'Multiphase electric machines for variable-speed applications', *IEEE Transactions on Industrial Electronics*, 2008, **55**, (5), pp. 1893–1909

[7] Bojoi, R., Rubino, S., Tenconi, A., Vaschetto, S.: 'Multiphase electrical machines and drives: a viable solution for energy generation and transportation electrification'. 2016 International Conference and Exposition on Electrical and Power Engineering (EPE), Iasi, Romania, 2016, pp. 632–639

[8] Cao, W., Mecrow, B.C., Atkinson, G.J., Bennett, J.W., Atkinson, D.J.: 'Overview of electric motor technologies used for more electric aircraft (MEA)', *IEEE Transactions on Industrial Electronics*, 2012, **59**, (9), pp. 3523–3531

[9] Jung, E., Yoo, H., Sul, S., Choi, H., Choi, Y.: 'A nine-phase permanent-magnet motor drive system for an ultrahigh-speed elevator', *IEEE Transactions on Industry Applications*, 2012, **48**, (3), pp. 987–995

[10] Duran, M.J., Levi, E., Barrero, F.: '*Multiphase electric drives: introduction*' (Wiley Encyclopedia of Electrical and Electronics Engineering, USA, 2017)

[11] Barrero, F., Duran, M.J.: 'Recent advances in the design, modeling, and control of multiphase machines – Part I', *IEEE Transactions on Industrial Electronics*, 2016, **63**, (1), pp. 449–458

[12] Duran, M.J., Barrero, F.: 'Recent advances in the design, modeling, and control of multiphase machines – Part II', *IEEE Transactions on Industrial Electronics*, 2016, **63**, (1), pp. 459–468

[13] Levi, E.: 'Advances in converter control and innovative exploitation of additional degrees of freedom for multiphase machines', *IEEE Transactions on Industrial Electronics*, 2016, **63**, (1), pp. 433–448

[14] Levi, E., Bodo, N., Dordevic, O., Jones, M.: 'Recent advances in power electronic converter control for multiphase drive systems'. 2013 IEEE Workshop on Electrical Machines Design, Control and Diagnosis (WEMDCD), Paris, France, 2013, pp. 158–167

[15] Bodo, N., Jones, M., Levi, E.: 'A space vector PWM with common-mode voltage elimination for open-end winding five-phase drives with a single DC supply', *IEEE Transactions on Industrial Electronics*, 2014, **61**, (5), pp. 2197–2207

[16] Daoud, M.I., Elserougi, A.A., Massoud, A.M., Bojoi, R., Abdel-Khalik, A.S., Ahmed, S.: 'Zero-/low-speed operation of multiphase drive systems with modular multilevel converters', *IEEE Access*, 2019, **7**, pp. 14353–14365

[17] White, D.C., Woodson, H.H.: '*Electromechanical Energy Conversion*' (John Willey and Sons, New York, 1959)

[18] Fortescue, C.L.: 'Method of symmetrical co-ordinates applied to the solution of polyphase networks', *Transactions of the American Institute of Electrical Engineers*, 1918, **XXXVII**, (2), pp. 1027–1140

[19] Clarke, E.: '*Circuit Analysis of A-C Power*' (John Willey and Sons, New York, 1941 -vol. 1- and 1950 -vol. 2-)

[20] Zhao, Y., Lipo, T.A.: 'Space vector PWM control of dual three-phase induction machine using vector space decomposition', *IEEE Transactions on Industry Applications*, 1995, **31**, (5), pp. 1100–1109

[21] Zoric, I., Jones, M., Levi, E.: 'Vector space decomposition algorithm for asymmetrical multiphase machines'. 19th International Symposium on Power Electronics (Ee), 2017, Novi Sad, Serbia, pp. 1–6

[22] Toliyat, H.A., Lipo, T.A., White, J.C.: 'Analysis of a concentrated winding induction machine for adjustable speed drive applications. II. Motor design and performance', *IEEE Transactions on Energy Conversion*, 1991, **6**, (4); pp. 684–692

[23] Pereira, L.A., Scharlau, C.C., Pereira, L.F.A., Haffner, J.F.: 'General model of a five-phase induction machine allowing for harmonics in the air gap field', *IEEE Transactions on Energy Conversion*, 2006, **21**, (4), pp. 891–899

[24] Levi, E.: '*Multiphase AC Machines (Chapter 3)*' in '*The Industrial Electronics Handbook: Power Electronics and Motor Drives*' (CRC Press, 2nd ed., Boca Raton, FL, 2011)

[25] Yepes, A.G., Riveros, J.A., Doval-Gandoy, J., Barrero, F., Lopez, O., Bogado, B., Jones, M., Levi, E.: 'Parameter identification of multiphase induction machines with distributed windings – Part 1: Sinusoidal excitation methods', *IEEE Transactions on Energy Conversion*, 2012, **27**, (4), pp. 1056–1066

[26] Riveros, J.A., Yepes, A.G., Barrero, F., Doval-Gandoy, J., Bogado, B., Lopez, O., Jones, M., Levi, E.: 'Parameter identification of multiphase induction machines with distributed windings – Part 2: Time-domain techniques', *IEEE Transactions on Energy Conversion*, 2012, **27**, (4), pp. 1067–1077

[27] Trzynadlowski, A.M.: '*Control of Induction Motors*' (Academic Press, USA, 2000)

[28] Che, H.S., Duran, M.J., Levi, E., Jones, M., Hew, W., Rahim, N.A.: 'Postfault operation of an asymmetrical six-phase induction machine with single and two isolated neutral points', *IEEE Transactions on Power Electronics*, 2014, **29**, (10), pp. 5406–5416

[29] Pellegrino, G., Bojoi, R.I., Guglielmi, P.: 'Unified direct-flux vector control for AC motor drives', *IEEE Transactions on Industry Applications*, 2011, **47**, (5), pp. 2093–2102

[30] Zheng, L., Fletcher, J.E., Williams, B.W., He, X.: 'A novel direct torque control scheme for a sensorless five-phase induction motor drive', *IEEE Transactions on Industrial Electronics*, 2011, **58**, (2), pp. 503–513

[31] Gao, L., Fletcher, J.E., Zheng, L.: 'Low-speed control improvements for a two-level five-phase inverter-fed induction machine using classic direct torque control', *IEEE Transactions on Industrial Electronics*, 2011, **58**, (7), pp. 2744–2754

[32] Duran, M.J., Prieto, J., Barrero, F., Riveros, J.A., Guzman, H.: 'Space-vector PWM with reduced common-mode voltage for five-phase induction motor drives', *IEEE Transactions on Industrial Electronics*, 2013, **60**, (10) pp. 4159–4168

[33] Blaschke, F.: 'The principle of field orientation as applied to the new transvector closed-loop system for rotating-field machines', *Siemens Review*, 1972, **34**, (3), pp. 217–220

[34] Singh, G.K., Nam, K., Lim, S.K.: 'A simple indirect field-oriented control scheme for multiphase induction machine', *IEEE Transactions on Industrial Electronics*, 2005, **52**, (4), pp. 1177–1184

[35] Che, H.S., Levi, E., Jones, M., Hew, W., Rahim, N.A.: 'Current control methods for an asymmetrical six-phase induction motor drive', *IEEE Transactions on Power Electronics*, 2014, **29**, (1), pp. 407–417

[36] Vukosavic, S.N., Jones, M., Levi, E., Varga, J.: 'Rotor flux oriented control of a symmetrical six-phase induction machine', *Electric Power Systems Research*, 2005, **75**, (2-3), pp. 142–152

[37] Khan, M.R., Iqbal, A., Ahmad, M.: 'MRAS-based sensorless control of a vector controlled five-phase induction motor drive', *Electric Power Systems Research*, 2008, **78**, (8), pp. 1311–1321

[38] Jones, M., Vukosavic, S.N., Dujic, D., Levi, E.: 'A synchronous current control scheme for multiphase induction motor drives', *IEEE Transactions on Energy Conversion*, 2009, **24**, (4), pp. 860–868

[39] Iffouzar, K., Taraft, S., Aouzellag, H., Ghedamsi, K., Aouzellag, D.: 'DRFOC of polyphase induction motor based on fuzzy logic controller speed'. 4th International Conference on Electrical Engineering (ICEE), Boumerdes, Algeria, 2015, pp. 1–7

[40] Zheng, L., Fletcher, J.E., Williams, B.W., He, X.: 'Dual-plane vector control of a five-phase induction machine for an improved flux pattern', *IEEE Transactions on Industrial Electronics*, 2008, **55**, (5), pp. 1996–2005

[41] Abdel-Khalik, A.S., Masoud, M.I., Williams, B.W.: 'Improved flux pattern with third harmonic injection for multiphase induction machines', *IEEE Transactions on Power Electronics*, 2012, **27**, (3), pp. 1563–1578

[42] Mengoni, M., Zarri, L., Tani, A., Parsa, L., Serra, G., Casadei, D.: 'High-torque density control of multiphase induction motor drives operating over a wide speed range', *IEEE Transactions on Industrial Electronics*, 2015, **62**, (2), pp. 814–825

[43] Parsa, L., Toliyat, H.A., Goodarzi, A.: 'Five-phase interior permanent-magnet motors with low torque pulsation' *IEEE Transactions on Industry Applications*, 2007, **43**, (1), pp. 40–46

[44] Wang, K., Zhu, Z.Q., Ombach, G.: 'Torque improvement of five-phase surface mounted permanent magnet machine using third-order harmonic' *IEEE Transactions on Energy Conversion*, 2014, **29**, (3), pp. 735–747

[45] Munim, W.N.W.A., Duran, M.J., Che, H.S., Bermudez, M., Gonzalez-Prieto, I., Rahim, N.A.: 'A unified analysis of the fault tolerance capability in six-phase induction motor drives', *IEEE Transactions on Power Electronics*, 2017, **32**, (10), pp. 7824–7836

[46] Gonzalez-Prieto, I., Duran, M.J., Barrero, F.: 'Fault-tolerant control of six-phase induction motor drives with variable current injection', *IEEE Transactions on Power Electronics*, 2017, **32**, (10), pp. 7894–7903

[47] Gonzalez-Prieto, I., Duran, M.J., Barrero, F., Bermudez, M., Guzman, H.: 'Impact of postfault flux adaptation on six-phase induction motor drives with parallel converters', *IEEE Transactions on Power Electronics*, 2017, **32**, (1), pp. 515–528

[48] Baneira, F., Doval-Gandoy, J., Yepes, A.G., López, Ó., Pérez-Estévez, D.: 'Control strategy for multiphase drives with minimum losses in the full torque operation range under single open-phase fault', *IEEE Transactions on Power Electronics*, 2017, **32**, (8), pp. 6275–6285

[49] Baneira, F., Doval-Gandoy, J., Yepes, A.G., López, Ó., Pérez-Estévez, D.: 'Comparison of postfault strategies for current reference generation for dual three-phase machines in terms of converter losses', *IEEE Transactions on Power Electronics*, 2017, **32**, (11), pp. 8243–8246

[50] Tani, A., Mengoni, M., Zarri, L., Serra, G., Casadei, D.: 'Control of multiphase induction motors with an odd number of phases under open-circuit phase faults', *IEEE Transactions on Power Electronics*, 2012, **27**, (2), pp. 565–577

[51] Kianinezhad, R., Nahid-Mobarakeh, B., Baghli, L., Betin, F., Capolino, G.A.: 'Modeling and control of six-phase symmetrical induction machine under fault condition due to open phases', *IEEE Transactions on Industrial Electronics*, 2008, **55**, (5), pp. 1966–1977

[52] Guzman, H., Duran, M.J., Barrero, F., Zarri, L., Bogado, B., Gonzalez-Prieto, I., Arahal, M.R.: 'Comparative study of predictive and resonant controllers in fault-tolerant five-phase induction motor drives', *IEEE Transactions on Industrial Electronics*, 2016, **63**, (1), pp. 606–617

[53] Takahashi, I., Noguchi, T.: 'A new quick-response and high-efficiency control strategy of an induction motor', *IEEE Transactions on Industry Applications*, 1986, **IA-22**, (5), pp. 820–827

[54] Depenbrock, M.: 'Direct self-control (DSC) of inverter-fed induction machine', *IEEE Transactions on Power Electronics*, 1988, **3**, (4), pp. 420–429

[55] Buja, G.S., Kazmierkowski, M.P.: 'Direct torque control of PWM inverter-fed AC motors – a survey', *IEEE Transactions on Industrial Electronics*, 2004, **51**, (4), pp. 744–757

[56] ABB Group: 'Direct torque control (DTC), a motor control technique for all seasons', available online: https://library.e.abb.com/public/0e07ab6a2de30809c1257e2d0042db5e/ABB_WhitePaper_DTC_A4_20150414.pdf, 2015.

[57] Casadei, D., Profumo, F., Serra, G., Tani, A.: 'FOC and DTC: two viable schemes for induction motors torque control', *IEEE Transactions on Power Electronics*, 2002, **17**, (5), pp. 779–787

[58] Hatua, K., Ranganathan, V.T.: 'Direct torque control schemes for split-phase induction machine', *IEEE Transactions on Industry Applications*, 2005, **41**, (5), pp. 1243–1254

[59] Yu, F., Zhang, X., Qiao, M., Du, C.: 'The direct torque control of multiphase permanent magnet synchronous motor based on low harmonic space vector PWM'. IEEE International Conference on Industrial Technology (ICIT), Chengdu, China, 2008, pp. 1–5

[60] Zhang, Z., Tang, R., Bai, B., Xie, D.: 'Novel direct torque control based on space vector modulation with adaptive stator flux observer for induction motors', *IEEE Transactions on Magnetics*, 2010, **46**, (8), pp. 3133–3136

[61] Gao, Y., Parsa, L.: 'Modified direct torque control of five-phase permanent magnet synchronous motor drives'. Twenty-Second Annual IEEE Applied Power Electronics Conference and Exposition (APEC), Anaheim, CA, USA, 2007, pp. 1428–1433

[62] Parsa, L., Toliyat, H.A.: 'Sensorless direct torque control of five-phase interior permanent-magnet motor drives', *IEEE Transactions on Industry Applications*, 2007, **43**, (4), pp. 952–959

[63] Taheri, A., Rahmati, A., Kaboli, S.: 'Comparison of efficiency for different switching tables in six-phase induction motor DTC drive', *Journal of Power Electronics*, 2012, **12**, (1), pp. 128–135

[64] Karampuri, R., Prieto, J., Barrero, F., Jain, S.: 'Extension of the DTC technique to multiphase induction motor drives using any odd number of phases'. IEEE Vehicle Power and Propulsion Conference (VPPC), Coimbra, Portugal, 2014, pp. 1–6

[65] Garcia-Entrambasaguas, P., Zoric, I., Gonzalez-Prieto, I., Duran, M.J., Levi, E.: 'Direct torque and predictive control strategies in nine-phase electric drives using virtual voltage vectors', *IEEE Transactions on Power Electronics*, 2019, available online. DOI: 10.1109/TPEL.2019.2907194

[66] Bermudez, M, Gonzalez-Prieto, I, Barrero, F, Guzman, H, Duran, M.J., Kestelyn, X.: 'Open-phase fault-tolerant direct torque control technique for five-phase induction motor drives', *IEEE Transactions on Industrial Electronics*, 2017, **64**, (2), pp. 902–911

[67] Bermudez, M., Gonzalez-Prieto, I., Barrero, F., Guzman, H., Kestelyn, X., Duran, M.J.: 'An experimental assessment of open-phase fault-tolerant virtual-vector based direct torque control in five-phase induction motor drives', *IEEE Transactions on Power Electronics*, 2018, **33**, (3), pp. 2774–2784

[68] Geyer, T.: '*Model Predictive Control of High Power Converters and Industrial Drives*' (Wiley, USA, 2016)

[69] Garcia, C.E., Prett, D.M., Morari, M.: 'Model predictive control: Theory and practice – a survey', *Automatica*, 1989, **25**, (3), pp. 335–348

[70] Kouro, S., Perez, M.A., Rodriguez, J., Llor, A.M., Young, H.A.: 'Model predictive control: MPC's role in the evolution of power electronics', *IEEE Industrial Electronics Magazine*, 2015, **9**, (4), pp. 8–21

[71] Cortes, P., Kazmierkowski, M.P., Kennel, R.M., Quevedo, D.E., Rodriguez, J.: 'Predictive control in power electronics and drives', *IEEE Transactions on Industrial Electronics*, 2008, **55**, (12), pp. 4312–4324

[72] Rodriguez, J., Cortes, P.: '*Predictive Control of Power Converters and Electrical Drives*' (Wiley-IEEE Press, USA, 2012)

[73] Vazquez, S., Rodriguez, J., Rivera, M., Franquelo, L.G., Norambuena, M.: 'Model predictive control for power converters and drives: Advances and trends', *IEEE Transactions on Industrial Electronics*, 2017, **64**, (2), pp. 935–947

[74] Rodriguez, J., Kazmierkowski, M.P., Espinoza, J.R., Zanchetta, P., Abu-Rub, H., Young, H.A., Rojas, C.A.: 'State of the art of finite control set model predictive control in power electronics', *IEEE Transactions on Industrial Informatics*, 2013, **9**, (2), pp. 1003–1016

[75] Gonzalez-Prieto, I., Zoric, I., Duran, M.J., Levi, E.: 'Constrained model predictive control in nine-phase induction motor drives', *IEEE Transactions on Energy Conversion*, 2019, available online. DOI: 10.1109/TEC.2019.2929622

[76] Barrero, F., Arahal, M.R., Gregor, R., Toral, S., Duran, M.J.: 'A proof of concept study of predictive current control for VSI-driven asymmetrical dual three-phase ac machines', *IEEE Transactions on Industrial Electronics*, 2009, **56**, (6), pp. 1937–1954

[77] Arahal, M., Barrero, F., Toral, S., Duran, M., Gregor, R.: 'Multi-phase current control using finite-state model-predictive control', *Control Engineering Practice*, 2009, **17**, (5), pp. 579–587

[78] Zou, J., Xu, W., Zhu, J., Liu, Y.: 'Low-complexity finite control set model predictive control with current limit for linear induction machines', *IEEE Transactions on Industrial Electronics*, 2018, **65**, (12), pp. 9243–9254

[79] Lim, C.S., Levi, E., Jones, M., Rahim, N.A., Hew, W.P.: 'FCS-MPC-based current control of a five-phase induction motor and its comparison with PI-PWM control', *IEEE Transactions on Industrial Electronics*, 2014, **61**, (1), pp. 149–163

[80] Lim, C., Levi, E., Jones, M., Rahim, N.A., Hew, W.: 'A comparative study of synchronous current control schemes based on FCS-MPC and PI-PWM for a two motor three-phase drive', *IEEE Transactions on Industrial Electronics*, 2014, **61**, (8), pp. 3867–3878

[81] Miranda, H., Cortes, P., Yuz, J.I., Rodriguez, J.: 'Predictive torque control of induction machines based on state-space models', *IEEE Transactions on Industrial Electronics*, 2009, **56**, (6), pp. 1916–1924

[82] Kennel, R., Rodriguez, J., Espinoza, J., Trincado, M.: 'High performance speed control methods for electrical machines: An assessment'. IEEE International Conference on Industrial Technology (ICIT), Vina del Mar, Chile, 2010, pp. 1793–1799

[83] Xie, W., Wang, X., Wang, F., Xu, W., Kennel, R.M., Gerling, D., Lorenz, R.D.: 'Finite-control-set model predictive torque control with a deadbeat solution for PMSM drives', *IEEE Transactions on Industrial Electronics*, 2015, **62**, (9), pp. 5402–5410

[84] Mamdouh, M., Abido, M.A., Hamouz, Z.: 'Weighting factor selection techniques for predictive torque control of induction motor drives: A comparison study', *Arabian Journal for Science and Engineering*, 2018, **43**, (2), pp. 433–445

[85] Riveros, J.A., Barrero, F., Levi, E., Duran, M.J., Toral, S., Jones M.: 'Variable speed five-phase induction motor drive based on predictive torque control', *IEEE Transactions on Industrial Electronics*, 2013, **60**, (8), pp. 2957–2968

[86] Fuentes, E.J., Silva, C.A., Yuz, J.I.: 'Predictive speed control of a two-mass system driven by a permanent magnet synchronous motor', *IEEE Transactions on Industrial Electronics*, 2012, **59**, (7), pp. 2840–2848

[87] Garcia, C., Rodriguez, J., Silva, C., Rojas, C., Zanchetta, P., Abu-Rub, H.: 'Full predictive cascaded speed and current control of an induction machine', *IEEE Transactions on Energy Conversion*, 2016, **31**, (3), pp. 1059–1067

[88] Rodriguez, J., Kennel, R.M., Espinoza, J.R., Trincado, M., Silva, C.A., Rojas, C.A.: 'High-performance control strategies for electrical drives: An experimental assessment', *IEEE Transactions on Industrial Electronics*, 2012, **59**, (2), pp. 812–820

[89] Duran, M.J., Riveros, J.A., Barrero, F., Guzman, H., Prieto, J.: 'Reduction of common-mode voltage in five-phase induction motor drives using predictive control techniques', *IEEE Transactions on Industry Applications*, 2012, **48**, (6), pp. 2059–2067

[90] Cortes, P., Rodriguez, J., Silva, C., Flores, A.: 'Delay compensation in model predictive current control of a three-phase inverter', *IEEE Transactions on Industrial Electronics*, 2012, **59**, (2), pp. 1323–1325

[91] Kouro, S., Cortes, P., Vargas, R., Ammann, U., Rodriguez, J.: 'Model predictive control – a simple and powerful method to control power converters', *IEEE Transactions on Industrial Electronics*, 2009, **56**, (6), pp. 1826–1838

[92] Arahal, M.R., Martin, C., Kowal, A., Castilla, M.d.M., Barrero, F.: 'Cost function optimization for multi-phase induction machines predictive control', *Optimal Control Applications and Methods*, 2019, pp. 1–10

[93] Aguilera, R.P., Acuña, P., Lezana, P., Konstantinou, G., Wu, B., Bernet, S., Agelidis, V.G.: 'Selective harmonic elimination model predictive control for multilevel power converters', *IEEE Transactions on Power Electronics*, 2017, **32**, (3), pp. 2416–2426

[94] Yuan, Q., Qian, J., Wu, H., Yin, W., Jiang, Q.: 'Stator current harmonic elimination control for the high-power synchronous motors with online implementation', *IET Power Electronics*, 2019, **12**, (4), pp. 801–809

[95] Azab, M., Awadallah, M.A.: 'Selective harmonic elimination in VSI-fed induction motor drives using swarm and genetic optimization', *International Journal of Power Electronics*, 2013, **5**, (1), pp. 56–74

[96] Wang, F., Davari, S.A., Chen, Z., Zhang, Z., Khaburi, D.A., Rodriguez, J., Kennel, R.: 'Finite control set model predictive torque control of induction machine with a robust adaptive observer', *IEEE Transactions on Industrial Electronics*, 2017, **64**, (4), pp. 2631–2641

[97] Cortes, P., Kouro, S., La Rocca, B., Vargas, R., Rodriguez, J., Leon, J.I., Vazquez, S., Franquelo, L.G.: 'Guidelines for weighting factors design in model predictive control of power converters and drives'. IEEE International Conference on Industrial Technology (ICIT), Churchill, Victoria, Australia, 2009, pp. 1–7

[98] Davari, S.A., Khaburi, D.A., Kennel, R.: 'An improved FCS–MPC algorithm for an induction motor with an imposed optimized weighting factor', *IEEE Transactions on Power Electronics*, 2012, **27**, (3), pp. 1540–1551

[99] Arahal, M.R., Barrero, F., Duran, M.J., Ortega, M.G., Martin, C.: 'Trade-offs analysis in predictive current control of multi-phase induction machines', *Control Engineering Practice*, 2018, **81**, pp. 105–113

[100] Martin, C., Bermudez, M., Barrero, F., Arahal, M.R., Kestelyn, X., Duran, M.J.: 'Sensitivity of predictive controllers to parameter variation in five-phase induction motor drives', *Control Engineering Practice*, 2017, **68**, pp. 23–31

[101] Rojas, C.A., Yuz, J.I., Silva, C.A., Rodriguez, J.: 'Comments on 'predictive torque control of induction machines based on state-space models'', *IEEE Transactions on Industrial Electronics*, 2014, **61**, (3), pp. 1635–1638

[102] Chai, S., Wang, L., Rogers, E.: 'Model predictive control of a permanent magnet synchronous motor with experimental validation', *Control Engineering Practice*, 2013, **21**, pp. 1584–1593

[103] Morel, F., Lin-Shi, X., Retif, J.M., Allard, B., Buttay, C.: 'A comparative study of predictive current control schemes for a permanent-magnet synchronous machine drive', *IEEE Transactions on Industrial Electronics*, 2009, **56**, (7), pp. 2715–2728

[104] Zhang, X., Hou, B., Mei, Y.: 'Deadbeat predictive current control of permanent magnet synchronous motors with stator current and disturbance observer', *IEEE Transactions on Power Electronics*, 2017, **32**, (5), pp. 3818–3834

[105] Siami, M., Khaburi, D.A., Abbaszadeh, A., Rodriguez, J.: 'Robustness improvement of predictive current control using prediction error correction for permanent magnet synchronous machines', *IEEE Transactions on Industrial Electronics*, 2016, **63**, (6), pp. 3458–3466

[106] Kwak, S., Moon, U.C., Clarke, J.C.: 'Predictive-control-based direct power control with an adaptive parameter identification technique for improved AFE performance', *IEEE Transactions on Power Electronics*, 2014, **29**, (11), pp. 6178–6187

[107] Young, H.A., Perez, M.A., Rodriguez, J.: 'Analysis of finite-control-set model predictive current control with model parameter mismatch in a three-phase inverter', *IEEE Transactions on Industrial Electronics*, 2016, **63**, (5), pp. 3100–3107

[108] Bogado, B., Barrero, F., Arahal, M.R., Toral, S., Levi, E.: 'Sensitivity to electrical parameter variations of predictive current control in multiphase drives' 39th Annual Conference of the IEEE Industrial Electronics Society (IECON), Vienna, Austria, 2013, pp. 5215–5220

[109] Sawma, J., Khatounian, F., Monmasson, E., Idkhajine, L., Ghosn, R.: 'Analysis of the impact of online identification on model predictive current control applied to permanent magnet synchronous motors', *IET Electric Power Applications*, 2017, **11**, (5), pp. 864–873

[110] Xia, C., Wang, M., Song, Z., Liu, T.: 'Robust model predictive current control of three-phase voltage source PWM rectifier with online disturbance observation', *IEEE Transactions on Industrial Informatics*, 2012, **8**, (3), pp. 459–471

[111] Chen, Z., Qiu, J., Jin, M.: 'Adaptive finite-control-set model predictive current control for IPMSM drives with inductance variation', *IET Electric Power Applications*, 2017, **11**, (5), pp. 874–884

[112] Yang, H., Zhang, Y., Liang, J., Xia, B., Walker, P.D., Zhang, N.: 'Deadbeat control based on a multipurpose disturbance observer for permanent magnet synchronous motors', *IET Electric Power Applications*, 2018, **12**, (5), pp. 708–716

[113] Davari, S.A., Khaburi, D.A., Wang, F., Kennel, R.M.: 'Using full order and reduced order observers for robust sensorless predictive torque control of induction motors', *IEEE Transactions on Power Electronics*, 2012, **27**, (7), pp. 3424–3433

[114] Rodas, J., Barrero, F., Arahal, M.R., Martín, C., Gregor, R.: 'On-line estimation of rotor variables in predictive current controllers: A case study using five-phase induction machines', *IEEE Transactions on Industrial Electronics*, 2016, **63**, (9), pp. 5348–5356

[115] Rodas, J., Martín, C., Arahal, M.R., Barrero, F., Gregor, R.: 'Influence of covariance-based ALS methods in the performance of predictive controllers with rotor current estimation', *IEEE Transactions on Industrial Electronics*, 2017, **64**, (4), pp. 2602–2607

[116] Martin, C., Arahal, M.R., Barrero, F., Duran, M.J.: 'Five-phase induction motor rotor current observer for finite control set model predictive control of stator current', *IEEE Transactions on Industrial Electronics*, 2016, **63**, (7), pp. 4527–4538

[117] Martin, C., Arahal, M.R., Barrero, F., Duran, M.J.: 'Multiphase rotor current observers for current predictive control: A five-phase case study', *Control Engineering Practice*, 2016, **49**, pp. 101–111

[118] Duran, M.J., Prieto, J., Barrero, F., Toral, S.: 'Predictive current control of dual three-phase drives using restrained search techniques', *IEEE Transactions on Industrial Electronics*, 2011, **58**, (8), pp. 3253–3263

[119] Luo, Y., Liu, C.: 'A simplified model predictive control for a dual three-phase PMSM with reduced harmonic currents', *IEEE Transactions on Industrial Electronics*, 2018, **65**, (11), pp. 9079–9089

[120] Geyer, T., Quevedo, D.E.: 'Multistep finite control set model predictive control for power electronics', *IEEE Transactions on Power Electronics*, 2014, **29**, (12), pp. 6836–6846

[121] Karamanakos, P., Geyer, T., Oikonomou, N., Kieferndorf, F.D., Manias, S.: 'Direct model predictive control: A review of strategies that achieve long prediction intervals for power electronics', *IEEE Industrial Electronics Magazine*, 2014, **8**, (1), pp. 32–43

[122] Arahal, M.R., Barrero, F., Duran, M.J., Martin, C.: 'Harmonic distribution in finite state model predictive control', *International Review of Electrical Engineering*, 2015, **10**, (2), pp. 172–179

[123] Barrero, F., Arahal, M.R., Gregor, R., Toral, S., Duran, M.J.: 'One-step modulation predictive current control method for the asymmetrical dual three-phase induction machine', *IEEE Transactions on Industrial Electronics*, 2009, **56**, (6), pp. 1974–1983

[124] Gregor, R., Barrero, F., Toral, S., Arahal, M.R., Prieto, J., Duran, M.J.: 'Enhanced predictive current control method for the asymmetrical dual-three phase induction machine', IEEE International Electric Machines and Drives Conference (IEMDC), Miami, FL, USA, 2009, pp. 265–272

[125] Gonzalez, O., Ayala, M., Rodas, J., Gregor, R., Rivas, G., Doval-Gandoy, J.: 'Variable-speed control of a six-phase induction machine using predictive-fixed switching frequency current control techniques', 9th IEEE International Symposium on Power Electronics for Distributed Generation Systems (PEDG), Charlotte, NC, USA, 2018, pp. 1–6

[126] Gonzalez-Prieto, I., Duran, M.J., Aciego, J.J., Martin, C., Barrero, F.: 'Model predictive control of six-phase induction motor drives using virtual voltage vectors', *IEEE Transactions on Industrial Electronics*, 2018, **65**, (1), pp. 27–37

[127] Xue, C., Song, W., Feng, X.: 'Finite control-set model predictive current control of five-phase permanent-magnet synchronous machine based on virtual voltage vectors', *IET Electric Power Applications*, 2017, **11**, (5), pp. 836–846

[128] Aciego, J.J., Gonzalez-Prieto, I., Duran, M.J.: 'Model predictive control of six-phase induction motor drives using two virtual voltage vectors', *IEEE Journal of Emerging and Selected Topics in Power Electronics*, 2019, **7**, (1), pp. 321–330

[129] Kazmierkowski, M.P., Krishnan, R., Blaabjerg, F.: '*Control in Power Electronics: Selected Problems*' (Academic Press Series in Engineering, USA, 2002)

[130] Volkov, A.V., Skal'ko, Y.S.: 'Optimal control over a variable-frequency asynchronous electric drive with SVI–PWM from the point of view of total power losses', *Russian Electrical Engineering*, 2008, **79**, (9), pp. 486–496

[131] Lemmens, J., Vanassche, P., Driesen, J.: 'Optimal control of traction motor drives under electrothermal constraints', *IEEE Journal of Emerging and Selected Topics in Power Electronics*, 2014, **2**, (2), pp. 249–263

[132] Xu, X., Novotny, D.W.: 'Selection of the flux reference for induction machine drives in the field weakening region', *IEEE Transactions on Industry Applications*, 1992, **28**, (6), pp. 1353–1358

[133] Kim, S.H., Sul, S.K.: 'Maximum torque control of an induction machine in the field weakening region', *IEEE Transactions on Industry Applications*, 1995, **31**, (4), pp. 787–794

[134] Kim, S.H., Sul, S.K.: 'Voltage control strategy for maximum torque operation of an induction machine in the field-weakening region', *IEEE Transactions on Industrial Electronics*, 1997, **44**, (4), pp. 512–518

[135] Harnefors, L., Pietilainen, K., Gertmar, L.: 'Torque-maximizing field-weakening control: design, analysis, and parameter selection', *IEEE Transactions on Industrial Electronics*, 2001, **48**, (1), pp. 161–168

[136] Kim, J.M., Sul, S.K.: 'Speed control of interior permanent magnet synchronous motor drive for the flux weakening operation', *IEEE Transactions on Industry Applications*, 1997, **33**, (1), pp. 43–48

[137] Cai, X., Zhang, Z., Wang, J., Kennel, R.: 'Optimal control solutions for PMSM drives: A comparison study with experimental assessments', *IEEE Journal of Emerging and Selected Topics in Power Electronics*, 2018, **6**, (1), pp. 352–362

[138] Levi, E., Dujic, D., Jones, M., Grandi, G.: 'Analytical determination of DC-bus utilization limits in multiphase VSI supplied AC drives', *IEEE Transactions on Energy Conversion*, 2008, **23**, (2), pp. 433–443

[139] Fall, O., Nguyen, N.K., Charpentier, J.F., Letellier, P., Semail, E., Kestelyn, X.: 'Variable speed control of a 5-phase permanent magnet synchronous generator including voltage and current limits in healthy and open-circuited modes', *Electric Power Systems Research*, 2016, **140**, pp. 507–516

[140] Bermúdez, M., Gomozov, O., Kestelyn, X., Barrero, F., Nguyen, N.K., Semail, E.: 'Model predictive optimal control considering current and voltage limitations: real-time validation using OPAL-RT technologies and five-phase permanent magnet synchronous machines', *Mathematics and Computers in Simulation*, 2019, **158**, pp. 148–161

[141] Bermúdez, M., Martín, C., Barrero, F., Kestelyn, X.: 'Predictive controller considering electrical constraints: a case example for five-phase induction machines', *IET Electric Power Applications*, 2019, available online. DOI: 10.1049/iet-epa.2018.5873

[142] Hoffmann, N., Andresen, M., Fuchs, F.W., Asiminoaei, L., Thøgersen, P.B.: 'Variable sampling time finite control-set model predictive current control for voltage source inverters'. IEEE Energy Conversion Congress and Exposition (ECCE), Raleigh, NC, USA, 2012, pp. 2215–2222

[143] Arahal, M.R., Martin, C., Barrero, F., Gonzalez-Prieto, I., Duran, M.J.: 'Model-based control for power converters with variable sampling time: A case example using five-phase induction motor drives', *IEEE Transactions on Industrial Electronics*, 2019, **66**, (9), pp. 5800–5809

[144] Arahal, M.R., Martin, C., Barrero, F., Duran, M.J.: 'Assessing variable sampling time controllers for five-phase induction motor drives', *IEEE Transactions on Industrial Electronics*, 2019, available online. DOI: 10.1109/TIE.2019.2908585

[145] Martin, C., Arahal, M.R., Barrero, F., Duran, M.J.: 'Model-based predictive current controllers in multiphase drives dealing with natural reduction of harmonic distortion', *Energies*, 2019, **12**.

[146] Trabelsi, M., Nguyen, N.K., Semail, E.: 'Real-time switches fault diagnosis based on typical operating characteristics of five-phase permanent-magnetic synchronous machines', *IEEE Transactions on Industrial Electronics*, 2016, **63**, (8), pp. 4683–4694

[147] Duran, M.J., Gonzalez-Prieto, I., Rios-Garcia, N., Barrero, F.: 'A simple, fast, and robust open-phase fault detection technique for six-phase induction motor drives', *IEEE Transactions on Power Electronics*, 2018, **33**, (1), pp. 547–557

[148] Gonzalez-Prieto, I., Duran, M.J., Rios-Garcia, N., Barrero, F., Martin, C.: 'Open-switch fault detection in five-phase induction motor drives using model predictive control', *IEEE Transactions on Industrial Electronics*, 2018, **65**, (4), pp. 3045–3055

[149] Guzman, H., Duran, M.J., Barrero, F., Bogado, B., Toral, S.: 'Speed control of five-phase induction motors with integrated open-phase fault operation using model-based predictive current control techniques', *IEEE Transactions on Industrial Electronics*, 2014, **61**, (9), pp. 4474–4484

[150] Guzman, H., Barrero, F., Duran, M.J.: 'IGBT-gating failure effect on a fault-tolerant predictive current controlled five-phase induction motor drive', *IEEE Transactions on Industrial Electronics*, 2015, **62**, (1), pp. 15–20

[151] Gonzalez-Prieto, I., Duran, M.J., Bermudez, M., Barrero, F., Martin, C.: 'Assessment of virtual-voltage-based model predictive controllers in six-phase drives under open-phase faults', *IEEE Journal of Emerging and Selected Topics in Power Electronics*, 2019, available online. DOI: 10.1109/JESTPE.2019.2915666

[152] Gonzalez-Prieto, I., Duran, M.J., Entrambasaguas, P., Bermudez, M.: 'Field oriented control of multiphase drives with passive fault-tolerance', *IEEE Transactions on Industrial Electronics*, 2019, available online. DOI: 10.1109/TIE.2019.2944056